Addis Ababa University

Addis Ababa Institute of Technology

Department of Electrical and Computer Engineering

Restoration of Voltage Collapse in Electric Power Network by Using Hybrid Predictive Control

Case Study: - On 230kV and 400kV Voltage level in Ethiopian Power Network

A thesis submitted to Addis Ababa Institute of Technology, School of
Graduate Studies, Addis Ababa University

in partial fulfillment of the requirement for the Degree of Master of Science in
Electrical Engineering (**Electrical Control Engineering**).

By

Mehari Mekuriaw Mengistie

Advisor: Dr. Solomon Kidane

Addis Ababa University
Addis Ababa Institute of Technology
Department of Electrical and Computer Engineering

Restoration of Voltage Collapse in Electric Power Network by Using Hybrid Predictive Control

Case Study: - On 230kV and 400kV Voltage level in Ethiopian Power Network

By Mehari Mekuriaw Mengistie

APPROVED BY BOARD OF EXAMINERS

_____	_____
Chairman, Department of Graduate Committee	Signature
Dr. SOLOMON KIDANE	_____
Advisor	Signature
_____	_____
Internal Examiner	Signature
_____	_____
External Examiner	Signature

ACKNOWLEDGEMENTS

First, I would like to thank my advisor, Dr. Solomon Kidane, for his support, understanding and encouragement during the whole work of this thesis. His advice played an important role in the completion of this work. He not only taught me valuable insights on conducting academic research but also gave me good instructions on career and life. I also want to express my gratitude to the rest of my program of study committee: Dr. Mengesha Mamo, Mr.libisework and Mr.Andinet. I greatly appreciate their valuable comments and advice on this work. Thank you very much for your contributions as members of my committee and efforts to help me improve my work.

Next, I would like to thank the Ethiopian Electric Power Corporation who gives valuable data to do this thesis and colleagues. I appreciate all their helps and friendships.

Last but not least, I would like to thank my father, my mother and my dear sisters and brothers. Their endless love and encouragement helped me through all these years.

_____

Mehari Mekuriaw Mengistie

TABLE OF CONTENTS

LIST OF TABLES

LIST OF FIGURES

LIST OF ABBREVIATIONS

EEPCo …….Ethiopian Electric Power Corporation

SCADA ……..Supervisory Control And Data Acquisition system

SSA ……Static Security Assessment

DSA ……Dynamic Security Assessment

DAE ……Differential Algebraic Equation

AGR…….Automatic Generator Regulators

SPS ……..System Protection Scheme

PMU…….Phase Measurement Unit

PDC ……....Phasor Data Concentrator

SE ……State Estimator

EEP……...Ethiopian Electric Power

EEU……..Ethiopian Electric Utility

MPC ……Model Predictive Control

ULTC..……..…Under Load Tap Changer

SVC …….……Static Var Compensators

OPF …….……..…Optimal Power Flow

LTC…….……..….Load Tap Changer

STATCOM…….…….….Static Compensator

PGEP ……..……..…Pseudo Gradient Evolutionary Programming

MIQP ……..……Mixed Integer Quadratic Programming

QSS …….……Quasi Steady-State

PSAT……...……..….Power System Analysis Toolbox

p.u. ……per unit

LIST OF NOTATIONS

$\sum$…….Summation

$\forall$ ……..For every (all)

$\in$ ……...Element of

$\| \|$……Magnitude

$\frac{\partial}{\partial}$ …….Partial derivative

η ……..Integration time step

Δ……Change in (difference)

Abstract

Ethiopia power network systems have been disturbed by unanticipated disturbances from time to time when numbers of consumers lose power supply at a very expensive cost. System protection and emergency control to respond this power system instability play an important role in our country power system operation. Driven by the industry need and improper protection mechanism to alleviate the effect of disturbances on system operation and improve power system security, this thesis uses a general framework for system protection scheme based on Model Predictive Control.

Model Predictive Control (MPC) is implemented to apply system protection scheme. A control strategy for maintaining voltage stability following the occurrence of an outage is stated. The result of our control mechanism on voltage recovery is measured via trajectory sensitivity. Our optimization means is mixed integer quadratic programming based algorithm is presented to study the optimal coordination of the dissimilar controls to advance voltage performance and effective use of control input following large disturbances.

The developed algorithms are functional with MATLAB and Power System Analysis Toolbox (PSAT) are joined and tested on the 30-bus of the 400kV and 230kV of the modified Ethiopia power network system for preventing voltage collapse and the objective of the algorithm is to attain its voltage level [0.95, 1.05 p.u] and filter out noise within the given prediction horizon.

Key Words: - Coordinated voltage control, model predictive control, trajectory sensitivity, power system.

CHAPTER 1. Overview

1.1 Background

Electricity holds a unique place in the world's infrastructure. It is a commodity, a technology and a necessity [1]. The electric power industry started with Edison Electric Illuminating Company and operated from 1882. Since then, the power industry has been evolving from none compatible, isolated multiple electric power companies, to interconnected bulk power systems [2]. But, Electric Power was introduced to Ethiopian in the late 19th Century, during the regime of Minilik in 1898. In the year 1948, an organization that had been formed with the power to administer an organization called Shewa Electric Power [3]. After many years it gains its current name Ethiopian Electric Corporation (EEPCo) in 1997. In 2014 it has divided into two which are Ethiopian Electric Power (EEP) and Ethiopian Electric Utility (EEU). The EEP is responsible for new construction of generation plant, transmission line and distribution system throughout Ethiopia. Both of them are a government owned but EEU responsible for the operation of generation, transmission, distribution and sales service of electric energy throughout Ethiopia, which is our focus area. The EEU has two electric power supply systems: the interconnected system (ICS) and the self-contained system (SCS) .The main energy source of ICS is hydropower plants, and for the SCS is mini-hydro and diesel power generators allocated in various parts of the country. The ICS consists of 11 hydro, one geothermal, two wind farms and 15 diesel power plants with a total capacity of above 2200MW, which most of is generated from hydropower plants. The SCS consists of three small hydro and many isolated diesel plants, located throughout the country with the capacity of almost 6.15MW and 30.06MW respectively.

The electric energy generated from the main hydropower plants is transported through high voltage transmission lines rated 45, 66, 132, 230 and 400kV. Regional interconnections with neighboring countries such as Djibouti and Sudan are done. Others like Kenya under construction and procurement phases.

The power distribution in both ICS and SCS is achieved at primary voltage of 33kV and 15kV lines, and step down to 380 and 220 volts to customer’s level. EEU increased the

number of electrified towns and villages reached to a total of 5163, which brought electric energy access to 54%.

It tackled many changes. This evolution is motivated by the pursuit of cheap and reliable electric power supply. The recent world major change of power industry from its vertically integrated anticompetitive structure to a deregulated competitive electric market structure but not in Ethiopian Electric Utility (EEU). The major consequence of the restructuring is the emergence of independent entities for generation, transmission, and distribution. A market structure for trading electrical energy has been developed based on the criteria of efficiency and reliability. According to the Ethiopian Electric Power Corporation, reliability has two aspects - adequacy and security. Security is the ability of the electric systems to withstand sudden disturbances such as electric short circuits or unanticipated loss of system elements. Therefore, to be reliable, the power system must be secure at most of time.

1.1.1 Power system Operating States

Based on the security level of a power system, its operating states are classified into normal state; alert state, emergency state, in extremis state and restorative state [4] as shown in Figure 1.1. This definition helps operators to design appropriate control actions for different operating conditions.

- **Normal state**: - In normal state, the power balance between generation and load is satisfied and no equipment is overloaded. All the voltages are within limits. In addition, the system has sufficient security margin to withstand any of the credible contingencies.
- **Alert state**: - Under this state, the power balance between generation and load is still met. No equipment is overloaded. No voltage is out of its limits. However, when a severe contingency occurs, the system will either have overloaded equipment's or has voltage violations.
- **Emergency state**: - The power balance between generation and load is still satisfied. However, either overload or voltage violation happens in emergency state. If suitable corrective control actions are taken, the state can still be restored to normal state or at least alert state.
- **In extremis state**:-Under this state, the power balance between generation and

load is lost. Voltage violation may happen and some equipment is overloaded. There are cascading outages. Load shedding may be taken to save as much of the system as possible.

- **Restorative state**: - Under this state, the operator performs control actions to restore all system loads. Depending on different cases, the system can reach either normal or alert state.

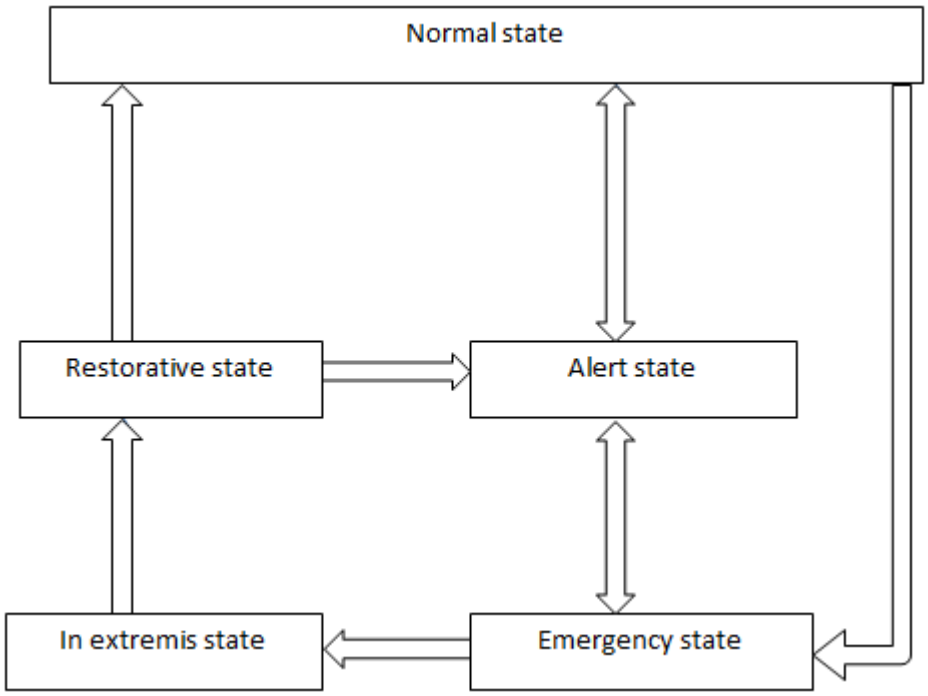

Figure 1.1 Power system operating state transition maps

1.1.2 Security assessment

The operation of a power system requires nearly strict synchronism of the rotational speed of many thousands of large interconnected generating units. Such operation requires not just the working of machine governors, but also all equipment operating within physical capabilities regardless of changes in customer demands or sudden disconnection of equipment from the system. Also due to economic consideration, a power system is operated close to its design limits, with smaller security margin and greater exposure to unacceptable conditions following disturbances. Security assessment plays an important role in system operation. It involves the evaluation of available data to approximate the relative security level

of present state or some near future state. According to [5], there are three levels of security assessment:

- **Security monitoring**:- Using measurements delivered by the supervisory control and data acquisition system (SCADA) and state estimation recognize whether the system is in normal state or not.
- **Security analysis**: - Security analysis is used to check the system's ability to withstand disturbances. If the system is in the normal state, contingency analysis is used to test the security of the system. If one or more operation constraints are violated in the contingency analysis, the system is insecure. Otherwise, it is secure.
- **Security margin determination**: - For a given operating condition, the determination of a security margin using some selected variables is used to measure the security level of a system. These margins are mainly needed in market environment. In this case, operators know how much load increase can be tolerable before the system becomes insecure.

Security assessment methods can be classified into two categories based on the different analysis methods: static Security Assessment (SSA) and dynamic security assessment (DSA).

- **Static Security Assessment (SSA):-** Static security can be seen as the ability of a power system, after a disturbance, to reach steady-state operating conditions without violating system constraints, which include limits on bus voltages and the thermal bounds of the line [6]. This analysis is usually based on power flow analysis. If operating conditions are not satisfactory with system constraints violation, preventive control or corrective control needs to be proposed to realize the following operation conditions
  1. No transmission line or other electric devices is overloaded.
  2. Bus voltages should be within their limits.
- **Dynamic Security Assessment (DSA)**:- Dynamic security analysis evaluates the power system's ability to resist a set of severe but credible contingencies and to survive transition to an acceptable steady-state

condition [7]. This involves the dynamic performance of generator models, dynamic load models, etc. A number of approaches to study dynamic stability have been developed, such as time domain simulation [8], direct method of transient stability analysis [8]. Besides dynamic security assessment study, different control strategies have also been proposed to improve the dynamic performances of power systems through load shedding actions, load tap changer actions, reactive power compensators and generator reference voltage settings.

1.1.3 Stability Analysis

The power system stability analysis has a big role in dynamic security assessment. Based on [9], power system stability is the ability of an electric power system, given initial operating condition, to regain a state of operating equilibrium after being exposed to a physical disturbance, with most system variables bounded so that practically the entire system remains stable. The power system is a highly nonlinear system and its stability is essentially a single problem. However, analysis of stability as well as planning methods to improve system operation performance can be greatly simplified by classification of stability into appropriate categories.

The classification of power system stability is based on the following considerations [10]:

- **The physical nature of the resulting mode of instability**:-rotor angle stability, frequency stability and voltage stability.
- **The size of the disturbance**:-small disturbance stability and large disturbance stability.
- **The time span**:-short-term stability and long term stability.

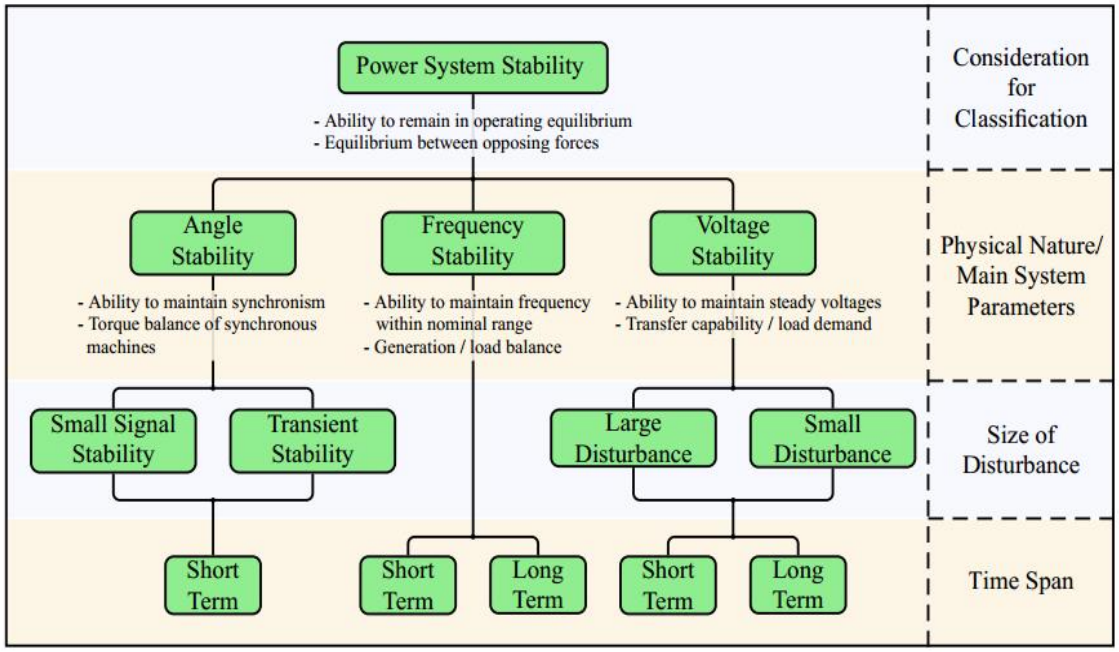

Figure 1.2 Classification of power system stability

Figure 1.2 shows the classification of power system stability [10]:-

- Rotor angle stability refers to the ability of synchronous machines to remain synchronism after a disturbance. The time frame of rotor angle stability analysis is from several seconds to 20 seconds
  - Small-disturbance rotor angle stability is the ability of a power system to remain synchronism under small disturbances. In today's power system, small-disturbance rotor angle stability results from the insufficient damping of oscillations. The analysis is based on the linearization of the nonlinear system equations at the steady operation point [10].
  - Large-disturbance rotor angle stability is the ability of the power system to remain synchronism when expose to a severe disturbance. Under a large disturbance, linearization of the system equation is not appropriate. The stability depends on the initial operating state of the system as well as the severity of the disturbance. The most common way to analyze system performance with a given initial point is time domain simulation, where a set of differential algebraic equations (DAEs) is solved.

- Voltage stability refers to the ability of a power system to maintain steady voltages at all buses after a disturbance with a given initial operating condition.
  - Large-disturbance voltage stability is the ability that a power system maintains steady voltages following large disturbances such as system faults, loss of transmission lines. The study of large-disturbance voltage stability is based on the nonlinear equations of generator models, load models; under load tap changer models, etc.
  - Small-disturbance voltage stability is the ability that a power system maintains steady voltages following small disturbances such as the fluctuation of loads. Under some assumptions, small-disturbance voltage stability can be analyzed by linearization of the nonlinear system equations. However, some nonlinear effect such as dead bands of tap changer controls cannot be taken into consideration. A combination of linear and nonlinear analyzes is used in voltage stability analysis [11].
  - Short-term voltage stability involves dynamics of induction motors. The time span for this analysis is several seconds.
  - Long-term voltage stability involves models such as under load tap changer, generator current limiters. The time span for the study ranges from several to many minutes [11].
- Frequency stability refers to the ability of a power system to maintain steady frequency after a severe system disturbance with a significant imbalance between generation and load. The period of time of interest for frequency ranges from fraction of seconds to several minutes. For a short-term phenomenon [12], the devices used for analysis are under frequency load shedding and generator controls and protections. The time span is fraction of seconds. For long-term frequency stability [13], the devices involve automatic generator regulators (AGR). The time span ranges from tens of seconds to several minutes.

1.1.4 Motivation

1.1.4.1 Traditional System Protection Scheme

A system protection scheme (SPS) is designed to sense abnormal system conditions and take predetermined, corrective action (other than the separation of faulted elements) to reservation system integrity and provide acceptable system performance [14]. System protection schemes came up as a compromise between investments, operation cost and customer service quality. They are smart mechanisms to improve system performance (stability, safety and security) due to their low economic costs and environmental openness when compared to the alternatives such as building new power plants and transmission lines. The most common SPS are probably triggered by either under frequency, under voltage, or high rate of change of frequency. These have been organized extensively in the Ethiopian national grid power system. However, these generally have local measurement, local processing and local actions. It was not economical to construct a new transmission line to alleviate this situation. Therefore, the design and implementation of a system protection schemes was carried out to dismiss the instability and overload system condition. Traditional system protection scheme is designed in off-line planning studies. It is implemented as shown in the figure 1.3 when it is triggered by some specific system operation condition in [14]. It consists of three main parts:

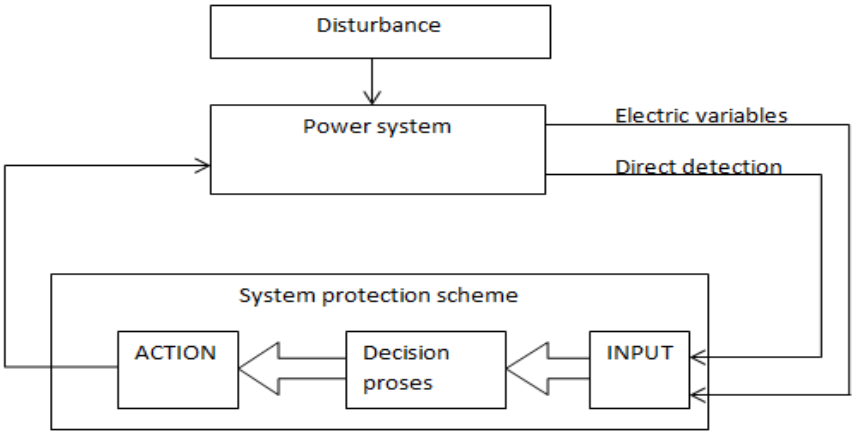

Figure 1.3 General Structure of a SPS

- Inputs (transmission line overload, status of circuits' breakers, etc.)
- A decision-making system that initiates certain actions based on the inputs
- Actions (such as generator or load tripping, capacitor switching, etc.)

According to input variables, SPS can be categorized into two categories: response-based SPS and event-based SPS. Response-based SPS uses power system operation condition to initiate control actions after the disturbance has caused the input variables significantly degraded. Under voltage load shedding and under frequency load shedding are two examples of this type of SPS. Event-based SPS is designed to activate control actions by the direct detection of a particular combination of events. This type of SPS is rule-based. Rules are established from on-line simulation. Examples of event-based SPS are load shedding or generator rejection by the tripping of a transmission line. Currently, Ethiopia also has this kind of protection for high voltage (HV) level in national grid of power system.

1.1.4.2 Real time System Protection Scheme

System protection schemes to resist load fluctuations and disturbances caused by faults are a vital part of an Ethiopian power system. Difference from the predetermined traditional SPS, the objective of a real time SPS is to carry out the control actions to mitigate the effects of potential instability or a safety/security degradation of a power system (such as a partial shutdown or a total collapse) noticed by an online dynamic security assessment program[15]. But the real time SPS is not implemented in the Ethiopia national grid power system. Since, in this thesis, the real time SPS propose to applied in our country power network system. Based on measurements received at control centers through high-speed communication channels and a system model, real time SPSs compute the necessary control decisions such as generator tripping, capacitor/reactor bank switching, transformer tap adjustments, and load-shedding for insecure contingencies. Recent advances in dynamic security assessment, monitoring, communication, and computing technologies have greatly facilitated the implementation of real time SPSs.

The functional structure of a real time SPS is shown in Figure 1.3[15]. Line flow measurements, bus voltage information; switch status measured by phase measurement units (PMUs) and collected by Phasor Data Concentrators (PDCs) are sent to a control

center through communication channels. These measurements plus a network model are used by the state estimator (SE) for filtering out the noise and estimating the auxiliary (also known as static state) variables. The results from the state estimator are used for power flow analysis. A power flow solution is then used by an on-line dynamic security assessment program to initialize the state variables of the dynamic models. Further, it uses system models and disturbance information to perform the contingency analysis to evaluate the security margin of the power system. If outage is identified where the system will become unstable, a real time system protection scheme should be designed to mitigate and relieve this situation.

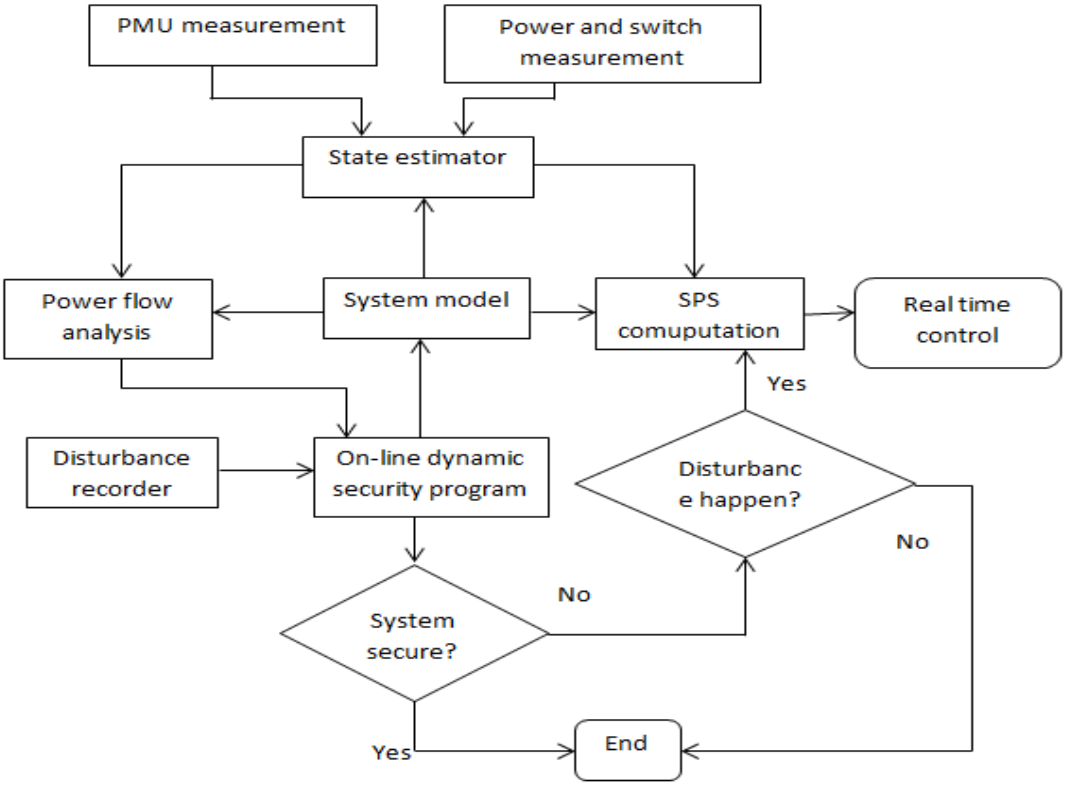

Figure 1.4 Structure of real time system protection scheme

The main motivation for the research work presented in this thesis is derived from the traditional system protection scheme drawbacks observed in the Ethiopian power system that are sever the network planners and operators as shown in the table 1.1 due to under voltage and voltage instability. The following are three major problems identified during the observation that require close attention:

Table 1.1 Sample of 2014 transmission outage report due to under voltage

ELEMENT NAME	OUTAGE		RESTORATION	
	Date	Time	Date	Time
230KV Shehedi - Gadarif Ckt-I	08/08/14	23:16	09/08/14	08:07
230KV Shehedi - Gadarif Ckt-II	08/08/14	23:16	09/08/14	08:07
230KV Gilgel Gibe-I - Sekoru Ckt-I	10/24/2014	16:16	10/24/2014	18:07
230KV Gilgel Gibe-I - Sekoru Ckt-II	10/24/2014	16:16	10/24/2014	18:07
230KV Shehedi - Gadarif Ckt-I	11/5/2014	12:30	11/5/2014	21:25
230KV Gefersa - Sululta Ckt-I	11/5/2014	12:58	11/5/2014	14:10
230KV Gefersa - Sululta Ckt-II	11/5/2014	12:58	11/5/2014	19:35

- It is not dynamic analysis i.e. no operator has the full view picture of what is happening in the given network.
- It is rule-based protection system lies on voltage, or their rate of change levels, or line flow limits. For example, if the measured voltage is lower than a specific value, or the line flow exceeds the line rating limit, a predefined SPS is triggered.
- It is based on local information which has not any system to measure and integrity the data at remote level.

All over the work however are based on static analysis, which means that the voltage performance criteria could be met only if the system reaches a post-contingency stable operating point. However, if the disturbances are severing, the power system may lose stability. Under this situation, the control strategy to restore the stable equilibrium point requires a dynamic analysis. Model predictive control (MPC) has been applied in Ethiopian power system voltage control based on dynamic analysis.

1.1.5 Objective of the thesis

1.1.5.1 General objective

The general objective of this thesis:

- To apply the model predictive control technique in Ethiopia electric power network system to improve the voltage stability performance and the system security.

1.1.5.2 Specific objective

The specific objectives of the thesis are:

1. To study mathematical model of Ethiopian power network system for voltage stability control design.
2. To analyze voltage stability after the fault occurred without any control mechanism in the Ethiopia power network system.
3. To analyze voltage stability after the fault occurred with coordinated control mechanism in the Ethiopian national grid.
4. To design model predictive control for voltage stability controls in Ethiopia power system with coordinated control mechanism.
5. To develop virtual reality of the Ethiopia power network system and evaluate performance of the propose control technique by using PSAT and MATLAB software.

1.1.6 Contribution of this Thesis

The research work presented in the thesis is inspired by the issues and problems tackled by system planners in managing acceptable system voltage and security in our case study . The following are the major novel contributions of this thesis:

i. It reviews the Ethiopian power network and its severing problem related with security.
ii. It states the model of 30-bus 230kV and 400kV voltage level Ethiopian national grid.
iii. It analysis the voltage stability after sever contingency occurred with and without coordinated control.
iv. It design model predictive control using trajectory sensitivity for the case of 30-bus 230kV and 400kV voltage level Ethiopian national grid and show that the voltage stability improvement with performance as well as satisfy system security.

1.1.7 Thesis organization

The rest of the thesis is organized as follows. Chapter 2 is a brief introduction of mathematical representation of power system models used in this thesis. Chapter 3 presents Model Predictive Control (MPC) based system protection scheme design methodology. A control strategy for maintaining voltage stability following the occurrence of a contingency is presented. Based on economic consideration and control effectiveness, a control switching strategy consisting of a sequence and amounts of coordinate control to switch is identified for voltage restoration. The effect of the coordinate control on voltage recovery is measured via trajectory sensitivity is presented in chapter 4. A mixed integer quadratic programming based algorithm is presented to study the optimal coordination of the dissimilar controls to improve voltage performance following large disturbances and mainly introduces the software realization of the MPC based control design. In chapter 5 also state the simulation result by using the developed algorithms are implemented with MATLAB and tested on the 30 bus Ethiopian system for preventing voltage collapse and voltage instability. The conclusion is given in Chapter 6.

CHAPTER 2. Power System Model

2.1 Overview

Power systems are large interconnected systems consisting of generation units, transmission grids, distribution systems and consumption units. The stability of a power system is dependent on several components, such as conventional generators and their exciters, dynamic loads and compensation devices. Therefore, an understanding of the characteristics of these devices and the modeling of their performances are of fundamental importance for stability studies and control design. There are numerous dynamics associated with a power system which may affect its stability.

To study the problem of modeling, all the components of a power system should be considered for their performance. Based on the requirements of stability study, different modeling schemes can be used for the same device; for example, three kinds of models of a system or device are necessary in order to study a power system's long term, midterm and transient stabilities.

The 230kV and 400kV Ethiopian power network as a test systems considered in this thesis consist of conventional generators, generator control systems including excitation control, transmission lines, transformers, reactive power compensation devices, under load tap changer transformer and loads of different kinds. Each piece of equipment has its own dynamic properties that may need to be modelled for a voltage stability study.

The dynamic behaviors of these devices are described through a set of nonlinear differential equations while the power flow in the network is represented by a set of algebraic equations. This gives rise to a set of differential-algebraic equations (DAEs) describing the behavior of a power system. Different types of models have been reported in the literature for each type of power system component depending upon its specific applications. In this chapter, the relevant equations governing the dynamic behaviors of the specific types of models used in this thesis are described.

2.2 Power System Network Model

The purpose of a power system is to deliver the power required by customers in real time with an acceptable quality. Power flow is used to analyze the steady state power system

operation condition [16]. The analysis is based on real and reactive power balance at each bus of a power grid. At bus *i*, the network model is described as follows:

$$0 = P_{Gi} - P_{Li} - P_{Ni} \tag{2.1}$$

$$0 = Q_{Gi} - Q_{Li} - Q_{Ni} \tag{2.2}$$

Where

- P_{Gi}: - real power generation injection at bus *i*
- Q_{Gi}: - reactive power generation injection at bus *i*
- P_{Li}: - real power load consumption at bus *i*
- Q_{Li}: - reactive power load consumption at bus *i*
- P_{Ni}: - net real power injection at bus *i*
- Q_{Ni}: - net reactive power injection at bus *i*

The output of real and reactive power of a generator is determined by the characteristics of the unit. The real and reactive power consumptions of a load are determined by the load characteristics. The net real and reactive power injections are constrained by the physical characteristics of a power grid as shown in figure 2.1, which are represented as:

$$P_{Ni} = \sum_{k=1}^{n} V_i V_k (G_{ik} \cos\theta_{ik} + B_{ik} \sin\theta_{ik}) \tag{2.3}$$

$$Q_{Ni} = \sum_{k=1}^{n} V_i V_k (G_{ik} \sin\theta_{ik} + B_{ik} \cos\theta_{ik}) \tag{2.4}$$

Where

- V_i: voltage magnitude of bus *i*
- V_k: voltage magnitude of bus k which is connected with bus *i*
- G_{ik}: conductance of the line from bus i to bus k
- B_{ik}: susceptance of the line from bus i to bus k
- θ_{ik}: voltage phase angular difference between bus i and bus k

Figure 2.1 Two Bus System

Operational considerations indicate that the active power P_{Gi} and the voltage magnitude V_i of a generator bus may be specified. For a load at bus i, the P_{Li} and Q_{Li} are also known. The power grid parameters G_{ik}; B_{ik} can be obtained by the network model. Therefore, power flow basically solves the nonlinear equation (2.3), (2.4) to obtain the steady states such as unknown bus voltage magnitude and phase angles of the power grid.

2.3 Synchronous Generator Model

The complete mathematical description of synchronous generators is too complicated to be used for system analysis and control design. Different degrees of approximations are used to simplify the generator model. In this thesis, two kinds of generator models are mentioned. One is the classical model, which is not applicable in our thesis; the other is the two-axis model, which is applicable in this thesis.

2.3.1 Classical Model

The classical model is the simplest model for generators (16). Following assumptions are adopted:

- Mechanical power input is constant
- q-axis transient voltage is constant

The differential equations for the classical model for generator i are as follows:

$$\dot{\delta} = \omega_i - \omega_s \tag{2.5}$$

$$M_i\dot{\omega}_i = P_{mi} - P_{ei} - D(\omega_i - \omega_s) \tag{2.6}$$

Where,

$$P_{ei} = \sum_{j=1}^{n} [E_i E_j B_{ij} \sin(\delta_i - \delta_j) + E_i E_j G_{ij} \cos(\delta_i - \delta_j)]$$

And

- δ_i: electrical rotor angle of generator i
- ω_i: rotor speed of generator i with respect to the synchronous frame
- ω_s: synchronous speed
- Mi: inertial constant of generator i
- P_{mi}: mechanical power input of generator i
- P_{ei}: electrical power output of generator i which is determined by interface equations between the generator i and power system network.
- D_i: damping coefficient

2.3.2 Two-axis Model

The Park-Concordia model is used for synchronous machine equations, whose scheme is depicted in Figure 2.2 which called the two-axis generator model accounts for the transient effects [17]. The mathematical formulation of generator i with this model is given by the following equations:

$$\dot{\delta} = \omega_i - \omega_s \tag{2.7}$$

$$\mathrm{M}_i \dot{\omega}_i = P_{mi} - (I_{di} E'_{di} + I_{qi} E'_{qi}) + (x'_{qi} - x'_{di}) I_{qi} I_{di} - D_i(\omega_i - \omega_s) \tag{2.8}$$

$$T'_{doi} \dot{E}'_{qi} = E_{fdi} - E'_{qi} - (x_{di} - x'_{di}) I_{di} \tag{2.9}$$

$$T_{qoi} \dot{E}'_{di} = -E'_{di} - (x_{qi} - x'_{qi}) I_{qi} \tag{2.10}$$

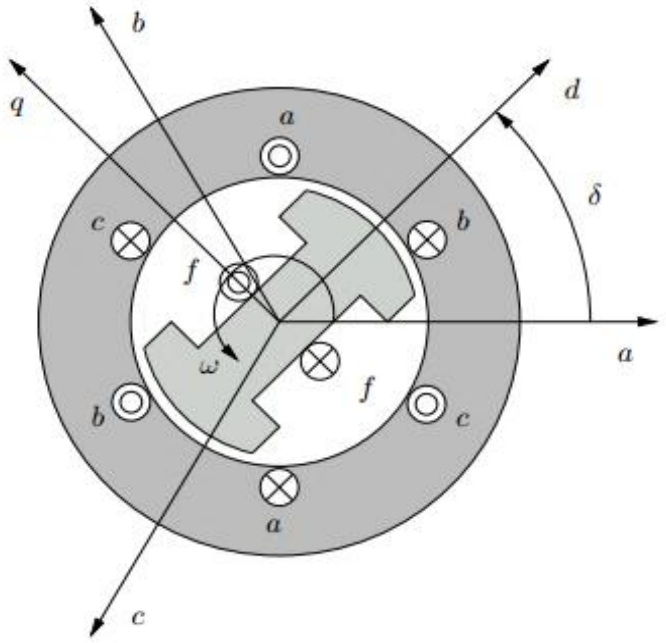

Figure 2.2 Synchronous machine scheme

Where,

- E_{di}' : Direct axes (d-axes) stator EMF corresponding to rotor transient flux components
- E_{qi}' : Quadrature axes (q-axes) stator EMF corresponding to rotor transient flux components
- I_d : The d-axes stator current
- I_q : The q-axes stator current
- T_{do}' : Open-circuit d-axes transient time constant
- T_{q0}' : Open-circuit q-axes transient time constant
- x_d, x'_d ,: d-axes synchronous and transient reactance
- x_q, x'_q ,: q-axes synchronous and transient reactance
- E_{fd} : Stator EMF corresponding to the field voltage

Interfaces of voltage equations to the power network are given by:

$$E'_{qi} = v_i \cos(\delta_i - \theta_i) + r_{ai} I_{qi} + x_{di}' I_{di} \tag{2.11}$$

$$E_{di}' = v_i \sin(\delta_i - \theta_i) + r_{ai} I_{di} + x_{qi}' I_{qi} \tag{2.12}$$

Where v and θ are bus voltage and angle, r_a is the machine armature resistance.

2.4 Excitation System Model

Different types of excitation system models used in power system are presented in [18]. In this thesis, we use the simplified IEEE type DC-1 excitation system as shown in Figure 2.3. The model is described by the following equations:

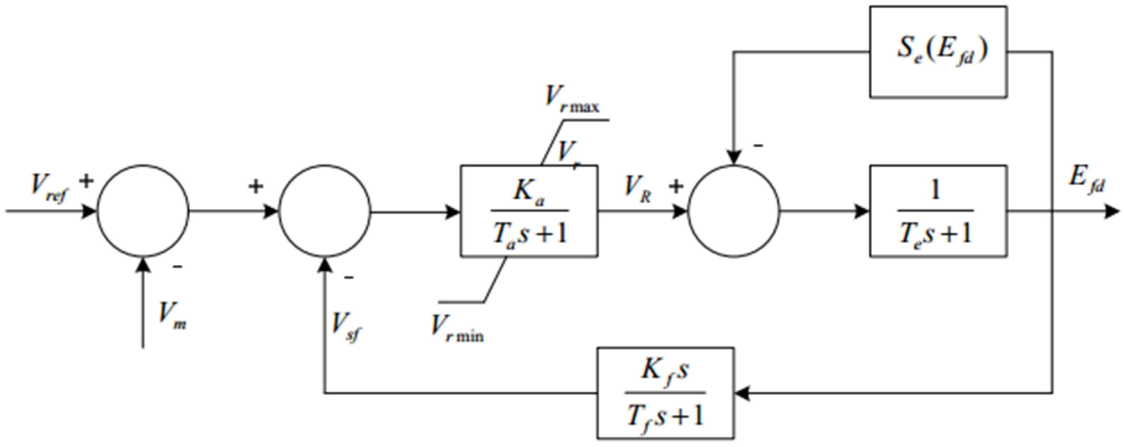

Figure 2.3 IEEE type DC-1 excitation system

$$T_a \dot{V}_r = (K_a (V_{ref} - V_m - V_{sf} - \frac{K_f}{T_f} E_{fd}) - V_r \tag{2.13}$$

$$T_f \dot{V}_{sf} = -(\frac{K_f}{T_f} E_{fd} + V_{sf}) \tag{2.14}$$

$$T_e \dot{E}_{fd} = -(E_{fd}(1 + S_e(E_{fd})) - V_R) \tag{2.15}$$

With

$$V_R = \begin{cases} V_r \ if \ V_{rmin} \le V_r \le V_{rmax}, \\ V_{rmin} \ if \ V_r < V_{rmin}, \\ V_{rmax} \ if \ V_r > V_{rmax}. \end{cases}$$

Where

- V_m: the voltage measurement value of the bus regulated by the generator
- V_{ref}: the reference voltage of the automatic voltage regulator (AVR)
- V_{sf}: the output of exciter soft feedback
- K_f: the gain of the exciter soft feedback
- T_f: the time constant of the exciter soft feedback
- K_a: the amplifier gain
- T_a: the amplifier time constant
- V_r : the non-windup output of AVR
- V_R: the windup output of AVR
- T_e: time constant of the exciter
- S_e: exciter saturation function which is a function of exciter output voltage E_{fd}

2.5 Load Model

Load dynamics has a significant effect on voltage performance following contingencies. A widely used dynamic load model, namely, exponential recovery load model, is presented in [18] and [19]. This model captures the physically observed behavior at high voltage buses. Moreover, it has been verified in several field tests for a wide range of operating conditions. In dynamic analysis, the active power consumption, denoted by P, is composed of two parts: the active power recovery P_r and the transient real power absorption P_t. The load model is expressed as follows

$$T_p \dot{P}_r = -P_r + P_s - P_t \tag{2.16}$$

$$P = P_r + P_t \tag{2.17}$$

Here, P_s and P_t are the static and transient real power absorptions, which depend on the load voltage:

$$P_s = P_0(V/V_0)^{\alpha_s} \tag{2.18}$$

$$P_t = P_0(V/V_0)^{\alpha_t} \tag{2.19}$$

T_P is the time taken for real power recovery to some specific value, which is also known as real power time constant.

Similar equations hold for the reactive power. Following a contingency, the reactive power consumption, denoted by Q, is composed of two parts: the reactive power recovery Q_r and the transient reactive power absorption

$$T_Q\dot{Q}_r = -Q_r + Q_s - Q_t \tag{2.20}$$

$$Q = Q_s + Q_t \tag{2.21}$$

Here, Q_s and Q_t are the static and transient reactive power absorptions, which depend on the load voltage.

$$Q_s = Q_0(V/V_0)^{\beta_s} \tag{2.22}$$

$$Q_t = Q_0(V/V_0)^{\beta_t} \tag{2.23}$$

T_Q is the time taken for reactive power recovery to some specific value, which is also called reactive power time constant.

2.6 Under Load Tap Changer

The equivalent ∏ circuit of the Under Load Tap Changer (ULTC) transformer is depicted in Figure 2.4. No magnetizing shunt is considered. The algebraic equations of the power injections are as follows:

$$
\begin{aligned}
P_k &= V_k^2(g_{km} + g_{k0}) - V_k V_m(g_{km}\cos\theta_{km} + b_{km}\sin\theta_{km}) \\
Q_k &= -V_k^2(b_{km} + b_{k0}) - V_k V_m(g_{km}\sin\theta_{km} - b_{km}\cos\theta_{km}) \\
P_m &= V_m^2(g_{km} + g_{m0}) - V_k V_m(g_{km}\cos\theta_{km} - b_{km}\sin\theta_{km}) \\
Q_m &= -V_m^2(b_{km} + b_{k0}) + V_k V_m(g_{km}\sin\theta_{km} + b_{km}\cos\theta_{km})
\end{aligned}
\qquad (2.24)
$$

Where $\Theta_{km} = \Theta_k - \Theta_m$; parameters g_{km}, b_{km}, b_{k0} and g_{k0} are functions of the tap ratio m and the transformer resistance r_T and reactance x_T, as follows:

$$
\begin{aligned}
g_{km} + jb_{km} &= \frac{m}{\bar{z}} \\
g_{k0} + jb_{k0} &= \frac{1-m}{\bar{z}} \\
g_{m0} + jb_{m0} &= \frac{m(m-1)}{\bar{z}}
\end{aligned}
\qquad (2.25)
$$

Where $z = r_T + jx_T$. Figure 2.5 depicts the UL TC control block diagrams. Two quantities can be controlled, i.e. the secondary voltage V_m and the reactive power Q_m .An under load tap changer (ULTC) transformer can be used to regulate a bus voltage. The mathematical representation of this continuous version of ULTC is represented by

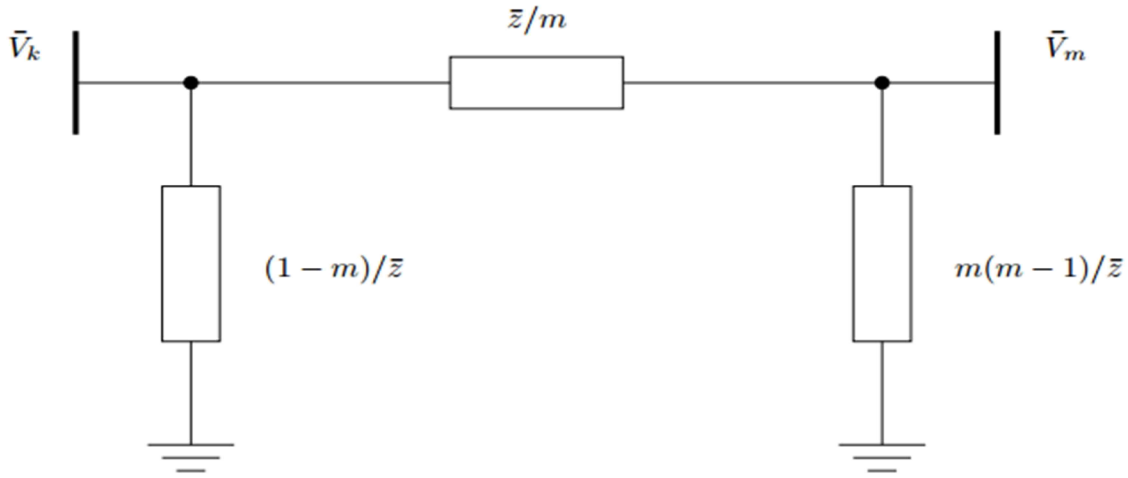

Figure 2.4 Under load tap changer: equivalent ∏ circuit

$$\dot{m} = -Hm + K(V_{reg} - V_{ref}) \qquad (2.26)$$

Where

- m: Tap ratio of ULTC transformer bank
- H: Integral deviation
- K: Inverse time constant

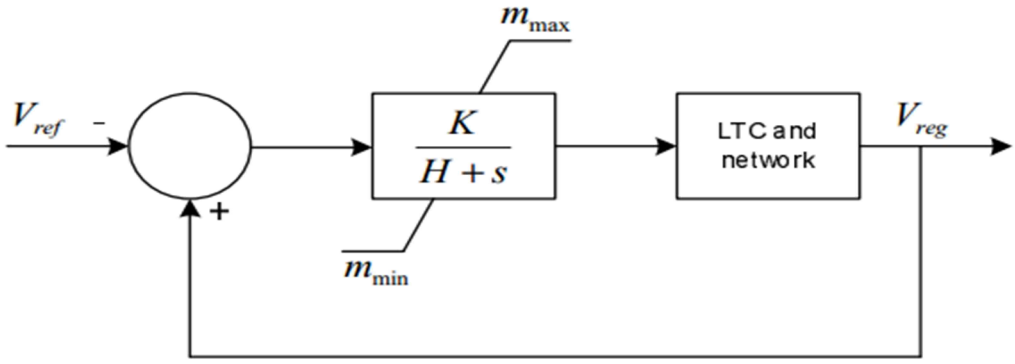

Figure 2.5 Under load tap changer voltage control

A discrete model of a ULTC is described as follows:

$$m_{k+1} = m_k + \Delta mR \tag{2.27}$$

Where

$$R=\begin{cases}1, & if\ u-u_{ref} > \Delta u,\\ -1, & if\ u-u_{ref} < -\Delta u,\\ 0, & if\ \|u-u_{ref}\| \le \Delta u.\end{cases}$$

- u: the voltage of the regulated bus
- u_{ref}: the reference voltage value of the regulated bus
- Δu: the error tolerance

2.7 Static Var Compensator (SVC)

The SVC regulators are implemented in the program which one assumes a time constant regulator, as depicted in Figure2.6. In this model, a total reactance b_{SVC} is assumed and the following differential equation holds

$$\dot{b}_{SVC} = (K_r(V_{ref} - V) - b_{SVC})/T_r \tag{2.28}$$

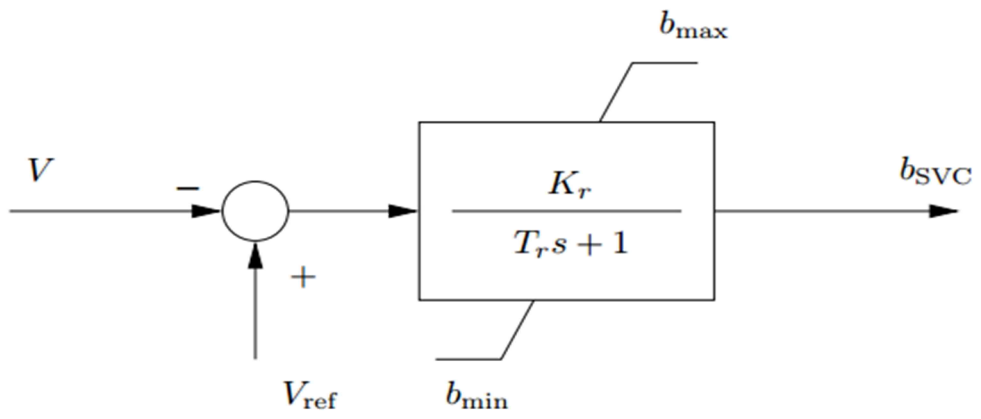

Figure 2.6 SVC Regulator

Where K_r is regulator, T_r is regulator time constant, V_{ref} is reference voltage. The model is completed by the algebraic equation expressing the reactive power injected at the SVC node:

$$Q = -b_{SVC} V^2 \tag{2.29}$$

The regulator has an anti-windup limiter, thus the reactance b_{SVC} is locked if one of its limits is reached and the first derivative is set to zero. The SVCs state variables are initialized after the power flow solution. To impose the desired voltages at the compensated buses, a PV generator with zero active power should be used. After the power flow solution the PV bus is removed and the SVC equations are used. During the state variable initialization a check for SVC limits is performed.

2.8 Power system Differential Algebraic Equation model

Through the above discussions, a complete power system model includes both dynamic model and static model. They are described by both differential equations and algebraic equations. Therefore, power system model can be represented by a set Differential Algebraic Equations (DAE).

$$\dot{x} = f(x, y) \tag{2.30}$$

$$0 = g(x, y) \tag{2.31}$$

The differential variables x represent the dynamic states associated with generators, excitation systems, and dynamic loads. The algebraic equation g represents the network power balance of power systems. The algebraic states y includes bus voltages magnitudes and bus phase angles.

In power system study, there also exist control variables and parameters. Therefore, Equation (2.30) and Equation (2.31) can also be written as Equation (2.32) and (2.33) to incorporate those variables. Vector u includes the control variables and parameters variable which may be used to control power system performance. In this thesis, the under load tap changer and shunt capacitor bank are treated as a discrete SVC are also treated as continuous which has the characteristics described in the above sections.

$$\dot{x} = f(x, y, u) \tag{2.32}$$

$$0 = g(x, y, u) \tag{2.33}$$

In power system modeling studies, the parameter values are chosen as either fixed values or within a certain range because the measurement of actual system parameters is very difficult. In particular, the load parameter values are difficult to obtain due to the large number of load components, the inaccessibility of certain customer loads, load compensation variations and the uncertainties of many load component characteristics.

This overall complete power modelling is applied in 30-bus 230kV and 400kV of Ethiopian power network system in the next chapter to improve voltage stability and similarly satisfied system security.

CHAPTER 3. Methodology

3.1 Overview

The system collapse may cause by voltage instability takes in bus voltages in a transmission system. Currently, voltage stability has become a major concern in power system planning and operation. Several factors have contributed to this situation. First, building new transmission facilities are more and more difficult because of the high capital investment and little or no right-of-way. Second, the construction of large, far-off power plants weakens the ability of voltage control and increases the electrical distance between load and generation. Third, the deregulation of power industry has created an economic inspiration to operate power systems closer to their limits. Voltage instability can occur under certain severe disturbances. Therefore, it is imperative that schemes for power system protection is in place to alleviate the shattering effects such as large scale shutdowns and collapses caused by such disturbances. This chapter studies voltage control strategies based on a model predictive control with control horizon. The control design includes:

- A formulation of a model predictive control based system protection scheme for maintaining voltage stability under emergencies.
- A formulation of a control strategy prevents voltage instability.
- A formulation of an optimal coordination of static var compensators (SVCs), transformer under load tap changers (ULTCs) and load shedding to improve voltage performance following large disturbances.

The unique features of our MPC formulation are as follows:

- Using of trajectory sensitivities for determining the effect of control on voltage stabilization, which is a more accurate way of determining the effectiveness of control.
- Optimization is performed repeatedly at each sampling instant. Only the first control step is implemented. This feature corrects the errors brought by model approximation, such as a linearized relationship between the voltages and the control variables.

- A decreasing horizon MPC is used. The control horizon decreases from one iteration to the next. This modification not only reduces the computation time, but also helps the convergence of the optimization process.
- Optimization performed at each step involves a quadratic cost function together with linear constraints, which makes the formulation scalable to large-sized practical systems (as demonstrated by the application to the 30 bus Ethiopian system).

3.2 Model Predictive Control

Model Predictive Control (MPC) is a class of algorithms that compute a sequence of control variable adjustments in order to optimize the future behavior of a plant (system). MPC was originally developed to meet the specialized control needs of petroleum refineries. Now it has been used in a wide variety of application areas including chemicals, food processing, automotive, aerospace, metallurgy, and power plants. A very general architecture of a Model Predictive Controller is given in Figure 3.1. MPC controller contains three basic functional blocks. The Optimizer finds the optimal control input u*(t) which when applied to the plant, gives the minimum value of the cost J. Of course, this optimization must be done in the presence of the constraints and the cost function. The State estimator is used to predict unmeasured states $\hat{x}(t)$ form the plant. An introduction to the basic concepts and formulations of MPC can be found in [20]. The principle of MPC is graphically depicted in Figure 3.2. Here *x* represents the state variable that needs to be controlled to a specific range. The available control is represented by variable *u*.

At a current time t_k, the MPC solves an optimization problem over a finite prediction horizon $[t_k, t_k + T_p]$ with respect to a predetermined objective function such that the predicted state variable $\hat{x}(t_k, T_p)$ can optimally stay close to a reference trajectory. The control is computed over a control horizon $[t_k, t_k + T_c]$, which is smaller than the

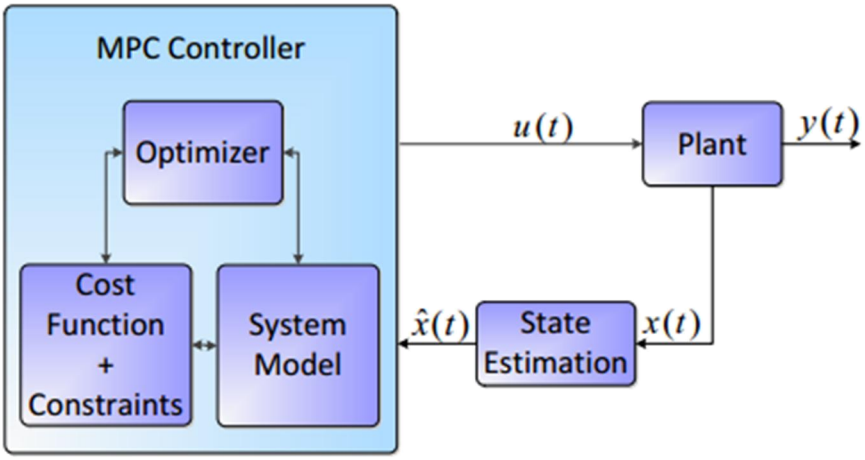

Figure 3.1 Model Predictive Controller block diagram

prediction horizon ($T_c \leq T_p$). If there were no disturbances, no model-plant mismatch and the prediction horizon is infinite, one could apply the control strategy found at current time t_k for all times $t \geq t_k$ .However, due to the disturbances, model-plant mismatch and finite prediction horizon, the true system behavior is different from the predicted behavior. In order to incorporate the feedback information about the true system state, the computed optimal control is implemented only until the next measurement instant ($t_k + T_s$), at which point the entire computation is repeated. In a MPC, the optimization problem to be solved at time t_k can be formulated as follows:

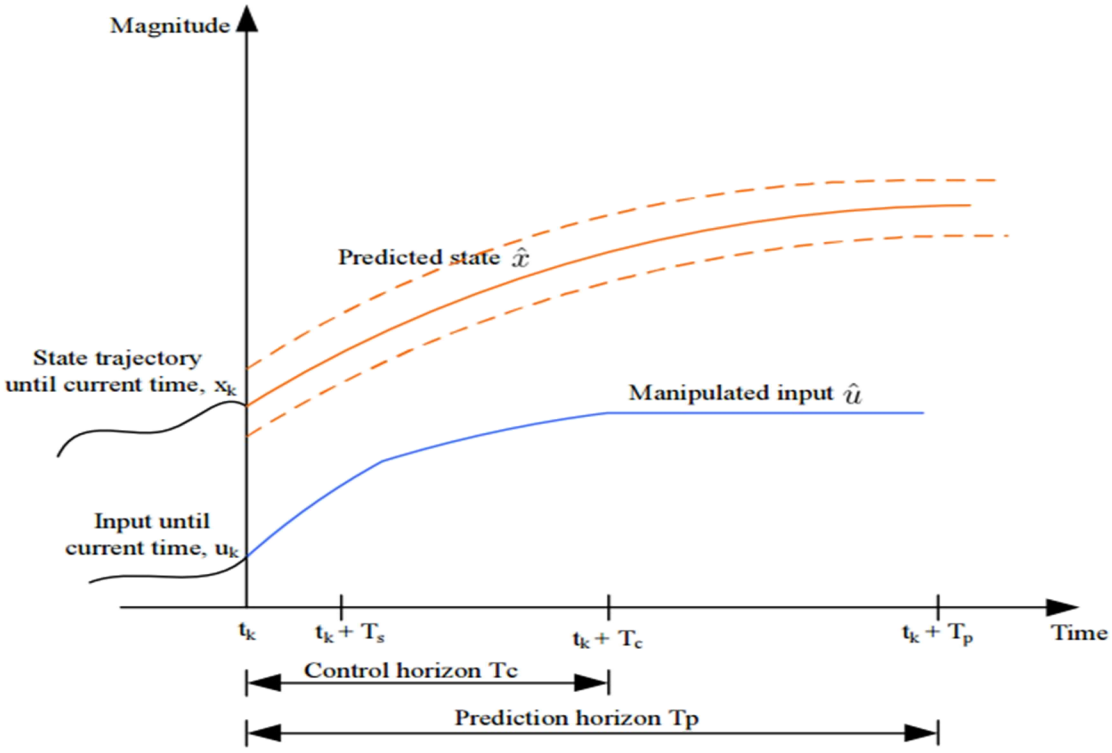

Figure 3.2 Principle of MPC

$$\min_{\hat{u}} \int_{t_k}^{t_k+T_P} F(\hat{x}(\tau),\hat{u}(\tau))d\tau \tag{3.1}$$

Subject to

$$\dot{\hat{x}}(\tau) = f(\hat{x}(\tau),\hat{u}(\tau)) \tag{3.2}$$

$$u_{\min} \le \hat{u} \le u_{\max}, \quad \forall \tau \in [t_k, t_k + T_C] \tag{3.3}$$

$$\hat{u}(\tau) = \hat{u}(t_k + T_C), \forall \tau \in [t_k + T_C, t_k + T_P] \tag{3.4}$$

$$x_{\min}(\tau) \le \hat{x}(\tau) \le x_{\max}(\tau), \forall \tau \in [t_k, t_k + T_P] \tag{3.5}$$

Here, T_c and T_p are the control and prediction horizon with $T_c \le T_p$. $\hat{x}$ denotes the estimated state and $\hat{u}$ represents "estimated" control (The true state may be different and the true control matches the estimated control only during the first sampling period).

Equation (3.1) represents the cost function of the MPC optimization. Equation (3.2) represents the dynamic system model with initial state x (t_k). Equations (3.3) and (3.4) represent the constraints on the control input during the prediction horizon. Equation (3.5) indicates the state operation requirement during the prediction horizon.

In the context of power systems, MPC has been applied mainly in two areas: voltage stabilization and frequency control. An emergency voltage control using tree search and model predictive control is presented in [21]. The emergency controls considered in the paper are: capacitor bank switching, tap changer operation and load shedding. The optimization objective is to minimize the deviation of the predicted voltage trajectory with respect to the reference trajectory as well as the weighted control cost. A special penalty is experienced when a constraint violation or a singularity induced bifurcation occurs. The paper mentions four different approaches to predict the system trajectory: nonlinear numerical simulation, Euler state prediction, off-equilibrium linearization, and Euler state prediction linear output approximation. The model predictive control is solved by an exhaustive tree search to compute a discrete-only control strategy.

In [22], a coordinated system protection scheme (SPS) against voltage collapse based on model predictive control and tree search is presented. Dissimilar and discrete controls such as generator voltage set-points, load-shedding, and tap-changers are coordinated. The objective function of the optimization includes: output deviation together with control and constraint violation costs. The prediction of the output trajectory is based on the linearization of the nonlinear system. The optimization is solved by exhaustive tree search. A Nordic test system is used to test the effectiveness of the scheme.

Model predictive control is also employed in [23], where an optimal coordinated voltage control for power system voltage stability is proposed. The controls used in the paper include: shunt capacitor banks, load shedding, and tap changers. The prediction of the output trajectory is based on the Euler state prediction. The main difference with the work reported in [21] lies in the method used for solving the MPC optimization problem. The optimization problem is solved by a pseudo gradient evolutionary programming (PGEP) technique, which allows computing optimal value for both discrete and continuous controls.

A method to compute an emergency voltage control strategy based on model predictive control is stated in [24]. The controls include tap changers, load shedding, and generator voltage set-points. The prediction of the output trajectories is based on trajectory sensitivity. While in the traditional model predictive control setting only the first control out of a sequence of computed control inputs is implemented, in the above papers the authors compute only an initial sequence of control inputs and implement it over the entire control horizon. The optimization problem is an example of mixed integer linear programming.

A voltage stabilization control strategy is proposed in [25] that are based on model predictive control and trajectory sensitivity. The control is exercised in form of load shedding. The objective function of the model predictive control is to minimize the amount of load shedding required to restore the voltages. The effectiveness of the load shedding on voltage restoration is established through trajectory sensitivity. The approach proposed in this recent work is questionably the most comprehensive, and the whole of the above work has stimulated the approach taken in the thesis.

3.3 Trajectory Sensitivity

Consider differential algebraic equations (DAEs) of a system,

$$\dot{x} = f(x, y, u), x(0) = x_0 \tag{3.6}$$

$$0 = g(x, y, u) \tag{3.7}$$

Where x is a vector of state variables, y is a vector of algebraic variables, and u is a vector of control variables. Trajectory sensitivity considers the influence of small variations in the control u (and any other variable of interest) on the solution of the state equations (3.6) and (3.7). Let u_0 be a nominal value of u, and assume that the nominal system in (3.8) and (3.9) has a unique solution x (t, x_0, u_0) over [t_0, t_1].

$$\dot{x} = f(x, y, u_0), x(0) = x_0 \tag{3.8}$$

$$0 = g(x, y, u_0) \tag{3.9}$$

Then the system in Equations (3.6) and (3.7) has a unique solution x (t, x_0, u) over [t_0, t_1] that is related to x (t, x_0, u_0) as:

$$x(t, x_0, u) = x(t, x_0, u_0) + x_u(t)(u - u_0) + high - order \ \ terms$$

$$y(t, x_0, u) = y(t, x_0, u_0) + y_u(u - u_0) + high - order \ \ terms$$

Here $x_u(t) = \dfrac{\partial x(t, x_0, u)}{\partial u}$ is called the trajectory sensitivities of state variables with respect to control variables u and $y_u = \dfrac{\partial y(t, x_0, u)}{\partial u}$ is the trajectory sensitivities of algebraic variables with respect to control variables u.

The evolution of trajectory sensitivities can be obtained by differentiating Equations (3.6) and (3.7) with respect to the control variables u and is expressed as:

$$\dot{x}_u(t) = f_x(t)x_u(t) + f_y(t)y_u(t) + f_u(t) \tag{3.10}$$

$$0 = g_x(t)x_u(t) + g_y(t)y_u(t) + g_u(t) \tag{3.11}$$

The trajectory sensitivity can be solved numerically. An efficient methodology is presented in (46) for the computation of trajectory sensitivities for a system represented by DAE equations. If the time domain simulation of a system is performed by the trapezoidal numerical integration approach, the trajectory sensitivity of state variables with respect to the small variations in initial state variables x and control variable u can be calculated as a byproduct of the time domain simulation. The x_u and y_u in Equation (3.10) and Equation (3.11) are part of the solution matrix.

Let

$$\bar{x} = \begin{bmatrix} x \\ u \end{bmatrix}, \bar{f} = \begin{bmatrix} f \\ 0 \end{bmatrix}$$

The DAE model (3.6) and (3.7) can be expressed as

$$\dot{\bar{x}} = \bar{f}(\bar{x}, y) \tag{3.12}$$

$$0 = \bar{g}(\bar{x}, y) \tag{3.13}$$

Trapezoidal approach is used to approximate Equation (3.12) with a set of algebraic difference equations coupled to the original algebraic Equation (3.13). The evolution of the states $\bar{x}$ and y from time instant t_i to the next time instant t_{i+1} can be described as:

$$\bar{x}^{i+1} = \bar{x}^i + \frac{\eta}{2}(\bar{f}(\bar{x}^{i+1}, y^{i+1}) + \bar{f}(\bar{x}^i, y^i)) \tag{3.14}$$

$$0 = g(\bar{x}^{i+1}, y^{i+1}) \tag{3.15}$$

Where superscript i is the time instant t_i, $i + 1$ is the time instant t_{i+1} and $\eta = t_{i+1} - t_i$ is the integration time step. Rearrange Equation 3.14 and Equation 3.15 as follows:

$$F = \begin{bmatrix} \frac{\eta}{2}\bar{f}(\bar{x}^{i+1}, y^{i+1}) - \bar{x}^{i+1} + \frac{\eta}{2}\bar{f}(\bar{x}^i, y^i) + \bar{x}^i \\ g(\bar{x}^{i+1}, y^{i+1}) \end{bmatrix} = 0 \tag{3.16}$$

Equation (3.16) is a set of implicit nonlinear algebraic equations. The Newton iterative technique is commonly used to solve for $\bar{x}^{i+1}$ and y^{i+1}, given $\bar{x}^{i}$ and y^{i} where, F_x is the Jacobian of F with respect to $\bar{x}$, y.

$$\begin{bmatrix} \bar{x}^{i+1} \\ y^{i+1} \end{bmatrix} = \begin{bmatrix} \bar{x}^{i} \\ y^{i} \end{bmatrix} - F_x^{-1} F$$

$$F_x = \begin{bmatrix} \frac{\eta}{2} \bar{f}_{\bar{x}} - I \frac{\eta}{2} \bar{f}_y \\ g_{\bar{x}} \qquad g_y \end{bmatrix}$$

Now consider the trajectory sensitivity equations. Differentiating Equations (3.12) and (3.13) with respect to the initial conditions $\bar{x}_0$ results in the DAEs of trajectory sensitivities

$$\dot{\bar{x}}_{\bar{x}_0} = \bar{f}_{\bar{x}} \bar{x}_{\bar{x}_0} + \bar{f}_y y_{\bar{x}_0} \tag{3.17}$$

$$0 = g_{\bar{x}} \bar{x}_{\bar{x}_0} + g_y y_{\bar{x}_0} \tag{3.18}$$

The trajectory sensitivity can be approximated by trapezoidal integration as follows:

$$\bar{x}^{i+1} = \bar{x}^{i}_{\bar{x}_0} + \frac{\eta}{2} (\bar{f}^{i}_{\bar{x}} \bar{x}^{i}_{\bar{x}_0} + \bar{f}^{i}_{y} y^{i}_{\bar{x}_0} + \bar{f}^{i+1}_{\bar{x}} \bar{x}^{i+1}_{\bar{x}_0} + \bar{f}^{i+1}_{y} y^{i+1}_{\bar{x}_0})$$

$$0 = g^{i+1}_{\bar{x}} \bar{x}^{i+1}_{\bar{x}_0} + g^{i+1}_{y} y^{i+1}_{\bar{x}_0}$$

Rearranging the above equation results in

$$\begin{bmatrix} \frac{\eta}{2} \bar{f}^{i+1}_{\bar{x}} - I \frac{\eta}{2} \bar{f}^{i+1}_{y} \\ g^{i+1}_{\bar{x}} \qquad g^{i+1}_{y} \end{bmatrix} \begin{bmatrix} \bar{x}^{i+1}_{\bar{x}_0} \\ y^{i+1}_{\bar{x}_0} \end{bmatrix} = \begin{bmatrix} -\frac{\eta}{2} (\bar{f}^{i}_{x_0} x^{i}_{\bar{x}_0} + \bar{f}^{i}_{y} y^{i}_{\bar{x}_0}) - \bar{x}^{i}_{\bar{x}_0} \\ 0 \end{bmatrix} \tag{3.19}$$

Therefore, the sensitivity matrix (3.20) can be obtained as a solution of a linear matrix equation. Notice that the coefficient matrix of Equation (3.19) is exactly the same as Jacobian matrix F_X in solving the for $\bar{x}^{i+1}$ and y^{i+1}. In our thesis, we extended the Power

System Analysis Tool [28] (a MATLAB based tool) to do trajectory sensitivity calculation and the MPC optimization.

$$\begin{bmatrix} \overline{x}_{\overline{x}_0}^{i+1} \\ y_{\overline{x}_0}^{i+1} \end{bmatrix} = \begin{bmatrix} x_{x_0} & x_{u_0} \\ u_{x_0} & u_{u_0} \\ y_{u_0} & y_{u_0} \end{bmatrix} \tag{3.20}$$

Figure 3.3 illustrates the application of trajectory sensitivity in evaluating the effect of controls on system behavior. The trajectory x_k of the nominal system represents the behavior under the control u_k. When the control is increased by Δu_1^k at time t_k, the change in predicted system behavior based on sensitivity analysis at time t_l, can be approximated as $\Delta x_1^{kl} = x_{u_1^k}^l \Delta u_1^k$. Here $x_{u_1^k}^l$ is the trajectory sensitivity of the state variable at time t_l with respect to the control at time t_k. Similarly if we increase the control by Δu_n^k at time $t_k + (n - 1)T_s$, the change in the state variable at time t_l is represented by $\Delta x_n^{kl} = x_{u_n^k}^l \Delta u_n^k$. Here, $x_{u_n^k}^l$ is the trajectory sensitivity of the state variable at time t_l with respect to the control at time $t_k + (n - 1)T_s$. Detailed information about trajectory sensitivity theory can be found in [27].

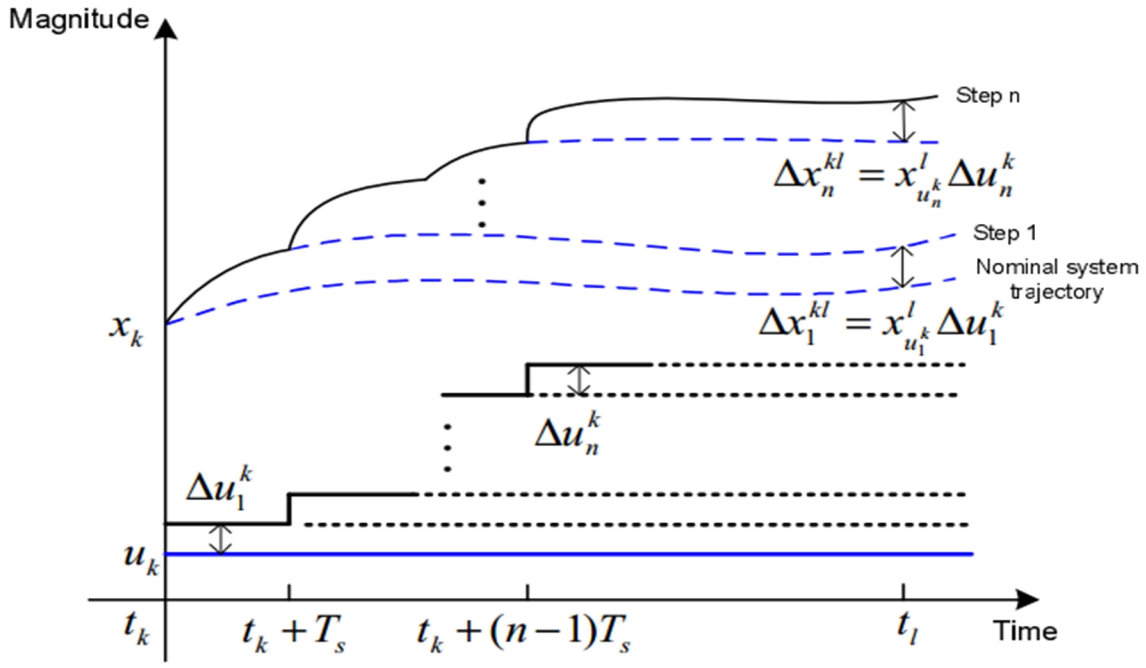

Figure 3.3 Application of trajectory sensitivity in system behavior prediction

3.4 Voltage Stability Margin

The security margin (voltage stability margin) of the computed optimal control strategy may not be satisfactory. In such a case, following the application of MPC based control, a small disturbance can result in a negative voltage stability margin and cause a voltage collapse. Hence there is a need to further extend the proposed design to account for the security margin (which must be greater than a pre-specified lower bound). In our work, voltage stability margin is adopted to indicate how secure power systems are. The sensitivities of the voltage stability margin on the controls are used to indicate the effectiveness of the controls on system security.

Voltage stability margin is an indication of how far the post-transient operating point is from the voltage collapse point. It is an index of system security. Consider a system with the DAE model

$$\begin{aligned} \dot{x} &= f(x,\ y,\ u,\ \lambda) \\ 0 &= g(x,\ y,\ u,\ \lambda) \end{aligned} \tag{3.21}$$

where x represents a vector of state variables, y represents a vector of algebraic variables, u is a vector of control variables and λ is a parameter.

Let $r(\lambda) \in \Re^{LX1}$ be a vector of variables which are parameterized by λ and a change in which (due to a change in λ) affects the system stability. (For the power system application, this will consist of load and generation power.) The l^{th} component of r(λ) is denoted as $r_l(\lambda)$ which increases linearly with λ as:

$$r_l(\lambda) = (1 + K_l\lambda) r_l(0) \tag{3.22}$$

Here, K_l is a constant and $r_l(0)$ represents the base case value of the l^{th} component of r(λ).

If λ increases slowly and continuously, a bifurcation point is reached beyond which the system loses stability. Let λ^* be the value of λ at this point, then this implies that

$$0 = f(x,\ y,\ u,\ \lambda),\ 0 = g(x,\ y,\ u,\ \lambda)$$

has no solution when $\lambda > \lambda^*$. The stability margin is defined as

$$SM = \sum_{l=1}^{l=L} (r_l(\lambda^*) - r_l(0)) = \lambda^* \sum_{l=1}^{l=L} K_l r_l(0) \tag{3.23}$$

The rate change of stability margin with respect to the control variable u is known as the margin sensitivity with respect to u:

$$SM_u = \frac{\partial SM}{\partial u} = \frac{\partial \lambda^*}{\partial u} \sum_{l=1}^{l=L} K_l r_l(0) \tag{3.24}$$

At the bifurcation point it holds that,

$$\frac{\partial \lambda^*}{\partial u} = -\frac{\omega^* F_u^*}{\omega^* F_\lambda^*} \tag{3.25}$$

where ω* is the left eigenvector corresponding to the zero eigenvalue of the system Jacobian

$F_x^* = [f_x^*, f_y^*; g_x^*, g_y^*]$; $F_\lambda^* = [f_\lambda^*; g_\lambda^*]$ is the derivative of system equations with respect to the bifurcation parameter λ; and $F_u^* = [f_u^*; g_u^*]$ is the derivative of system equations to the control variable u. (A variable superscripted with * denotes the value of that variable at the bifurcation point.)

In a power system, the voltage stability margin can also be defined based on this concept. For this, the real power P_l at bus l corresponds to the l^{th} component of r (λ) and satisfies

$$P_l = (1 + K_{lp}) P_{l0} \tag{3.26}$$

where P_{l0} is the base case real power load at bus l and K_{lp} is the gain factor characterizing the real power increase pattern. λ is known as loading parameter. Then the *voltage stability margin*, defined as the distance between the current operating point and the bifurcation point, can be expressed as:

$$SM = \sum_{l=1}^{L} P_l^* - \sum_{l=1}^{L} P_l = \lambda^* \sum_{l=1}^{L} K_{lp} P_l \tag{3.27}$$

A continuation power flow method is presented in (47) to trace the bifurcation point, through which the voltage stability margin can be calculated. Figure 3.3 shows voltage stability margin of a nominal system. This figure shows the change of voltage with respect to the increase of total real power consumption when load increases gradually in the system. Suppose under normal condition, the system has a total system load indicated in Figure 3.4. The voltage stability margin SM is defined as the difference between the total load at the voltage collapse point and that of the nominal system.

The *voltage stability margin sensitivity* SM_u with respect to the control variable u is given by,

$$SM_u = \frac{\partial SM}{\partial u} = \frac{\partial \lambda^*}{\partial u} \sum_{l=1}^{L} K_{lp} P_{l0} \tag{3.28}$$

Where $\frac{\partial \lambda^*}{\partial u}$ can be calculated by Equation (3.25). A detailed derivation of the sensitivity calculation is presented in (48).

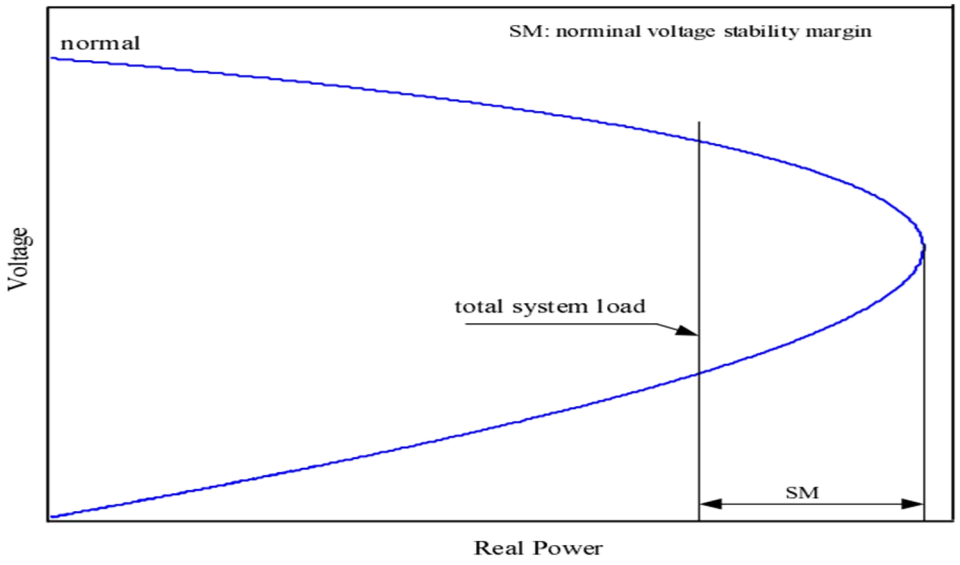

Figure 3.4 Voltage stability margin illustrations

In order to design a protection scheme involving the system security requirement, voltage stability margin sensitivity will be used to determine the influence of control on voltage stability.

CHAPTER 4. Controller Design

4.1 Introduction

Power systems operate close to their capacity limit as a result of deregulation as well as demand increase. While power systems are designed with proper planning and with proper stability margin, the instability can still occur under certain severe disturbances, and it is imperative that schemes for power system protection be in place to alleviate their catastrophic effects such as large scale shutdowns and collapses.

Controlling of the production, absorption, and flow of reactive power at various locations in the system means controlling of the voltage level in the system. With regard to a power system, sources and/or sinks of reactive power, such as shunt capacitors, shunt reactors, synchronous condensers, and static var compensators (SVCs) are used to control voltage level. In literature, many algorithms have been developed to maintain a satisfactory voltage profile. A detailed study of on-line voltage/var control performed on the Ontario Hydro system is presented in [28]. The objective function is to minimize the transmission loss as well as the amount of controls. An optimal power flow (OPF) formulation is adopted to schedule generator voltages and transformer tap positions in the bulk transmission system. Furthermore, the frequency of the generator voltages and transformer tap changers to be optimized is studied to achieve most of the possible transmission loss savings. An optimal power flow based real time voltage control method is proposed in [29]. The primary goal is to eliminate voltage violations. However, under conditions where violations can not be removed, the objective is to minimize violations. Under the normal operating condition where all the voltages are satisfactory, the objective is to minimize system losses. The controls include transformer tap changers and generator voltage set-points. Besides the OPF based voltage control, Artificial Intelligence especially expert system has also been applied in the study. [30] develops an expert system to assist the decision-making of power system in presence of a voltage violation problem. Empirical rules are generated to mitigate voltage problem using tap changers, reactive injections, and generator voltage setting points. The proposed approach is composed of four steps: identification of the knowledge required to solve a selected problem, justification of the identified empirical rules, development of

production rules and testing and modification. The sensitivity of voltage magnitude change with respect to various controllers is used to evaluate the maximum voltage increase with the available control. A rule-based approach for decentralized voltage control is presented in [31]. A network decomposition technique is used to alleviate a bus voltage limit violation. Only the local information local to the bus with a voltage violation is adopted in control decision making. Network voltage sensitivity with respect to the available voltage controllers is calculated and a rule-based approach is developed to select the optimal set of control actions for alleviating voltage violations. The controls include generator voltage setpoints, reactor switching and tap changers. Distributed expert systems are developed in [32] for voltage control. The controls is composed of load shedding, shunt capacitors, tap changers, static var compensator as well as load flow control. Each var compensating device is controlled by a dedicated computer. An expert system is designed in each computer. Communication exists among those computers. Contribution degree is defined to evaluate the ability of a control in restoring voltages. In [33] two rule-based techniques in a voltage control expert system are introduced. Reactive path concept is adopted to determine control regions of each reactive power compensator and efficient controllers for each observed bus. The decision is based on two sets of rule-based techniques. All the above work is based on static analysis, in which only the real and reactive power balance in each bus of a power system is considered. The power system is assumed to have a stable operating point. The voltage performance criteria could be met only if the system reaches a post-contingency stable operating point. However, if disturbances are sever, the power system may lose stability. Under this situation, the control strategy to restore the stable equilibrium point requires a dynamic analysis. The dynamic behavior of system components such as dynamic load characteristics, dynamic behavior of load tap changers need to be taken into account. In this section, we propose computation of the optimal strategies considering the dynamic behavior of a power system based on model predictive control (MPC). The voltage problem is a local as well as a regional problem. One approach to study the coordinated voltage control is based on system response. In other words, direct telemetry of voltage at power system pivot nodes are used as feedback to design voltage control. This approach are popular in European countries and some south American countries. The coordinated

control falls into three hierarchical levels: primary voltage control, secondary voltage control and tertiary voltage control according to the control response time and effective scale [34]. The hierarchical levels are illustrated by Figure 4.1.

The primary control level basically is related with unit and plant control. The units in a power plant usually are connected to a power grid through step-up transformers. Automatic voltage regulators (AVRs) directly installed on generators can be used to control generator terminal voltage. This control can also be applied to maintain the high-side voltage of step-up transformers equal to specific values to avoid reactive power interchange among plant units. Primary actions are very fast, in a time frame of few seconds. It is considered as a local control. The secondary voltage control level is to adjust and to maintain the voltage profile inside a network area. Control actions in this level include var compensation devices like capacitors, inductors, synchronous or static voltage compensators and transformer load tap changers. Definition and implementation of secondary voltage control level are quite dependent on philosophy of each utility. The time frame for secondary control is from several seconds to minutes. It is considered a regional control. The purpose of tertiary voltage control level is to increase the system's operating security

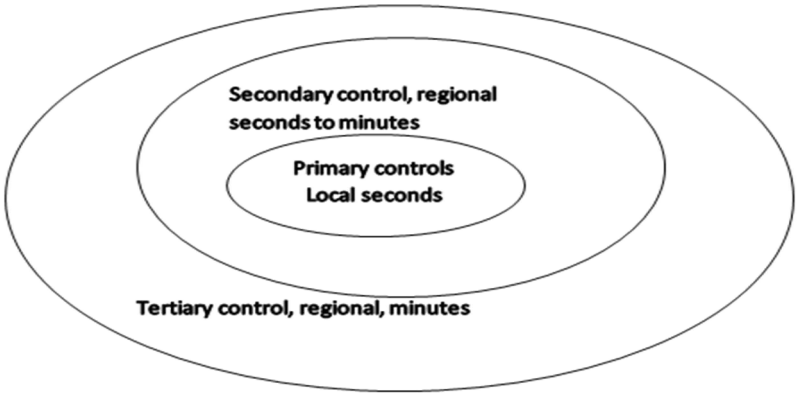

Figure 4.1 Hierarchical voltage control levels

and efficiency through centralized coordination of the decentralized secondary voltage controllers. The time scale of this control is several minutes or on demand. The characteristics of the hierarchical coordinated voltage control system applied on the Italian transmission grid are introduced in [36, 35]. The power plants adjust their reactive

power output based on the voltage measured at pivot nodes. The hierarchical coordinated control scheme was studied on the French electrical system [34]. Spain [37], Belgium [38] as well as Brazil [39] have experiences to apply the secondary voltage control. Besides industry applications, some research work has been done on the response based coordinated voltage control. The work is based on static analysis. A knowledge based system for supervision and control of regional voltage profile and security using fuzzy logic is presented in [40]. It involves the coordination of AVRs, shunt capacitors as well as the high-side voltage set points at power plants. Besides the response based control design, there also exists model based coordination control design. The motivation of model based coordination control design lies in the fact that local measurement sometime can not reffect the global system behavior. An example is provided in [27] to illustrate this situation. Paserba et. al. [41] discussed the coordination of distribution-level load tap changers (LTCs), mechanically-switched capacitors and static compensators (STATCOMs) to improve voltage profile and to reduce the mechanical switching operations within the substation. Park et. al. [42] proposed a coordinated control method for LTCs and capacitors in distribution systems to reduce power loss and to improve the voltage profile during a day. Kim et. al. [43] presented an artifficial neural network based coordination control scheme for LTCs and STATCOMs to minimize the amount of transformer tap changes and STATCOM outputs while maintaining acceptable voltage magnitudes at substation buses. The above work is based on power system steady state analysis. Some work has also been done to design a coordinated voltage control strategy by considering dynamic response of a power system. Larsson et. al. [44] presented a method of coordination of load shedding, capacitor switching and tap changers using model predictive control. The prediction of states is based on the numerical simulation of nonlinear differential algebraic equations (DAEs) directly and Euler state prediction. A tree search method is adopted to solve the optimization. Larsson et. al. [45] proposed a coordination of generator voltage set-points, load shedding and LTCs using a heuristic search and the predictive control. The prediction of states is based on the linearization of nonlinear DAEs. Wen et. al. [23] presented an optimal coordinated voltage control using model predictive control. The controls used include: shunt capacitors, load shedding, tap changers and generator voltage set-points. The prediction of voltage trajectory is based

on the Euler state prediction. The optimization problem is solved by a pseudo gradient evolutionary programming (PGEP) technique. Zima et. al. [24] presented a coordinated voltage control by using tap changers, load shedding, and generator voltage setting points The prediction of the voltage trajectories is based on trajectory sensitivity. The optimization is solved by a mixed integer program. In this section, we design a coordinated control of SVCs, LTCs and load shedding to improve voltage performance following disturbances. Given the locations and capabilities of SVCs, LTCs and interruptible load, the control design problem is to determine the control sequences and the control amounts to satisfy voltage performance requirements. MPC with a decreasing control horizon is adopted in the control design. At each MPC iteration, a mixed integer quadratic programming (MIQP) problem is solved. The objective function is to minimize a weighted sum of the cumulative voltage deviations and the cumulative cost of the coordinated controls. Trajectory sensitivities are used to estimate the effect of controls on voltage trajectories. The decreasing control horizon MPC not only reduces the computation time, but also greatly helps the convergence of the optimization process. The iterative optimization process of MPC helps ensure that errors introduced due to trajectory sensitivities and any model inaccuracies are minimized.

4.2 Problem Formulation and Solution

The importance of this work is to determine an optimal coordinated control strategy consisting of continuous and discrete power system controls to improve voltage performance and prevent voltage instability. If the occurrence of a certain pre-identified contingency is noticed and the system performance is not satisfactory, for instance, voltages are out of the their limits, an optimal coordinated control strategy is identified based on a decreasing horizon MPC algorithm consisting of the amount and sequence of dissimilar voltage control equipments such as SVCs, transformer tap changers and load shedding. The control changes only at the sampling instants.

Let T_p be the prediction horizon, T_c be the control horizon, T_s be the control sampling interval, and $N = \frac{T_c}{T_s}$ be the total number of control steps. The procedure to determine the control strategy at the k[th] sampling instant is as follows:

Step 1:- At time t_k(i.e. the (k + 1)[th] sampling instant), an estimate of the current state $x(t_k)$ is obtained. The nominal power system evolves according to Equations (3.6) and (3.7).

$$\dot{x} = f(x, y, u_c, u_d), x(0) = x_0 \tag{4.1}$$

$$0 = g(x, y, u_c, u_d) \tag{4.2}$$

Here, $u_c = \left\{ C_m^0 + \sum_{i=0}^{k-1} \Delta C_{m1}^i \right\}_{m=1}^{m=M_c}$ is the continuous control variable (e.g. amounts of SVC currently in use). C_m^0 is the amounts of continuous variables that exist at time 0. $\sum_{i=0}^{k-1} \Delta C_{m1}^i$ is the amounts of the continuous variable that were added over time[0, t_k - T_s]. $u_d = \left\{ D_m^0 + \sum_{i=0}^{k-1} S_{m1}^i \Delta D_{m1}^i \right\}_{m=M_{c+1}}^{m=M_c+M_d}$ is the discrete control amount. D_m^0 is the amounts of discrete variables that exist at time 0. $\sum_{i=0}^{k-1} S_{m1}^i \Delta D_{m1}^i$ is the amount of the discrete control that were added over time [0, t_k - T_s]. Here, S_{m1}^i is the step size of the discrete actuator m at sampling point t_i, and ΔD_{m1}^i is the number of steps of the discrete actuator at time t_i.

Time domain simulation is used to obtain the trajectory of the nominal system (4.1) and (4.2), starting from the state $x(t_k)$ at time t_k to the end of prediction horizon $t_k + T_p$. At the same time, the trajectory sensitivities of bus voltages with respect to the continuous and discrete controls to be added at instants $t_k + (n - 1)T_s$; $n = 1 \ldots N$ - k are obtained and denoted as $V_{C_{mn}}^{kj}(t)$; $V_{D_{mn}}^{kj}(t)$ (see below for the explanation of notation).

Step 2:- At time t_k, solve the quadratic integer programming optimization problem over the prediction horizon $[t_k, t_k + T_p]$ and a control horizon $[t_k, t_k + (N - k)Ts]$ as stated in (4.3)-(4.10).

Minimize with respect to ΔC_{mn}^{k} and ΔD_{mn}^{k}

$$\int_{t_k}^{t_k+T_p}(\hat{V}^k(t)-V_{ref})'R(\hat{V}^k(t)-V_{ref})dt+\sum_{m=1}^{m=M_c}\sum_{n=1}^{n=N-K}W_{mn}\Delta C_{mn}^{k}+\sum_{m=M_c+1}^{m=M_c+M_d}\sum_{n=1}^{n=N-K}W_{mn}S_{mn}^{k}\Delta D_{mn}^{k} \quad (4.3)$$

Subject to

$$\Delta C_{\mathrm{m}}^{\min}\le\Delta C_{mn}^{k}\le\Delta C_{m}^{\max}, \quad (4.4)$$

$$\Delta D_{m}^{\min}\le\Delta D_{mn}^{k}\le\Delta D_{m}^{\max}, \quad (4.5)$$

$$C_{m}^{\min}\le C_{m}^{0}+\sum_{i=0}^{k-1}\Delta C_{m1}^{i}+\sum_{n=1}^{N-K}\Delta C_{mn}^{k}\le C_{m}^{\max}, \quad (4.6)$$

$$D_{m}^{\min}\le D_{m}^{0}+\sum_{i=0}^{k-1}S_{m1}^{i}\Delta D_{m1}^{i}+\sum_{n=1}^{N-K}S_{mn}^{k}\Delta D_{mn}^{k}\le D_{m}^{\max}, \quad (4.7)$$

$$V_{\min}^{kj}(t)\le V^{kj}(t)+\sum_{m=1}^{M_c}\sum_{n=1}^{N-k}V_{C_{mn}}^{kj}\Delta C_{mn}^{k}+\sum_{m=M_c+1}^{M_c+M_d}\sum_{n=1}^{N-k}V_{D_{mn}}^{kj}(t)S_{mn}^{k}\Delta D_{mn}^{k}\le V_{\max}^{kj}(t) \quad (4.8)$$

$$SM^{k-1}+\sum_{m=1}^{M_c}SM_{C_m}^{k}(\sum_{n=1}^{N-k}\Delta C_{mn}^{k})+\sum_{m=M_c+1}^{M_c+M_d}SM_{D_m}^{k}(\sum_{n=1}^{N-k}S_{mn}^{k}\Delta D_{mn}^{k})\ge SM_{D} \quad (4.9)$$

$$\Delta C_{mn}^{k}\ge 0, m=1,...,M_c \quad (4.10)$$

ΔD_{mn}^{k} is an integer, m=M_c +1,…,M_c +M_d (4.11)

Here,

- R is the weighting matrix.
- $\hat{V}^k(t)$ is the voltage vector at time $t \in [t_k, t_k + T_P]$ as predicted at the sampling instant t_k.
- W_{mn} is the weight for the cost of control m to be added at time $t_k+ (n -1)T_s$.
- M_c is the total number of continuous control variables, i.e. the number of available SVCs.

- M_d is the total number of discrete control variables, i.e. the number of available under load tap changer plus the number of load shedding candidate locations.
- N is the total number of control steps.
- ΔC_{mn}^{k} is the amount of continuous actuator m to be added at time $t_k + (n-1)T_s$ in iteration k.
- ΔD_{mn}^{k} is the number of steps of discrete actuator m to be added at time $t_k + (n-1)T_s$ in iteration k. It is an integer.
- S_{mn}^{k} is the step size of discrete actuator m at time $t_k + (n-1)T_s$ in iteration k.
- $\Delta C_{m}^{\min} \in \Re$ is the minimum amount of continuous control m to be added at control sampling points, typically 0.
- $\Delta C_{m}^{\max} \in \Re$ is the maximum amount of continuous control m to be added at control sampling points.
- $\Delta D_{m}^{\min} \in \Re$ is the minimum number of steps of discrete control m to be added at control sampling points, typically 0.
- $\Delta D_{m}^{\max} \in \Re$ is the maximum number of steps of discrete control m to be added at control sampling points.
- ΔC_{m1}^{i} is the amount of control m implemented at the control sampling point t_i ; i =0,…, k- 1.
- $C_{m}^{\min} \in \Re$ is the minimum amount of continuous control m that must be used, typically 0.
- $C_{m}^{\max} \in \Re$ is the maximum available amount of continuous control m.
- $D_{m}^{\min}$ is the minimum amount of discrete control m.
- $D_{m}^{\max}$ is the maximum available amount of discrete control m.
- $V^{kj}(t) \in \Re$ is the voltage of bus j at time $t(t_k \le t \le t_k + T_p)$ of the nominal system at time t_k.
- $V_{\min}^{kj}(t)$ is the minimum voltage at bus j desired at time $t_k \le t \le t_k + T_p$.

- $V_{\max}^{kj}(t)$ is the maximum voltage at bus j desired at time $t_k \le t \le t_k + T_p$.
- $V_{C_{mn}}^{kj}(t)$ is the trajectory sensitivity of the voltage at bus j at time $t_k \le t \le t_k + T_p$ with respect to the continuous control m added at time $t_k + (n-1)T_s$.
- $V_{D_{mn}}^{kj}(t)$ is the trajectory sensitivity of the voltage at bus j at time $t_k \le t \le t_k + T_p$ with respect to the discrete control m added at time $t_k + (n-1)T_s$.
- SM^{k-1} is the voltage stability margin at time $t_k - T_s$.
- $SM_{C_m}^{k}$ is the stability margin sensitivity with respect to continuous control m added at time t_k.
- $SM_{D_m}^{k}$ is the stability margin sensitivity with respect to discrete control m added at time t_k.
- SM_D is the desirable stability margin for the system.

The objective of the optimization is to minimize the voltage deviation and cumulative cost of continuous and discrete controls as shown in Equation (4.3). Equation (4.4) constraints the amount of the continuous control m to be added at time $t_k + (n-1)T_s$. Equation (4.5) is the control step constraints on discrete actuators. Equation (4.6) constraints the total amount of continuous control m to be added over $[t_k, t_k + (N-k)T_s]$. Equation (4.7) constraints the total amount of discrete control m to be added over $[t_k, t_k + (N-k)T_s]$. Equation (4.8) shows constraints the voltage fluctuation at time $t \in [t_k, t_k + T_p]$. Equation (4.9) shows the stability margin constraint for both discrete and continuous case. The number of candidate control locations and their upper limits are determined through a prior planning step. The total number of control variables in the optimization is the number of candidate control locations times the number of control steps. The optimization problem is solved in Matlab, and it does converge to a global minimum.

Step 3:- At time t_k, the solution of the optimization problem (4.3)-(4.11) computes a sequence of controls ΔC_{mn}^{k} and ΔD_{mn}^{k}. Add only the first control ΔC_{m1}^{k} and $S_{m1}^{k}\Delta D_{m1}^{k}$ at time t_k and obtain the system state $x(t_{k+1})$ at time $t_{k+1} = t_k + T_s$.

Step 4:- Increase k to k + 1 and repeat steps (1)-(3) until k = N - 1.

4.3 Software Development

4.3.1 Overview

Power System Analysis Toolbox (PSAT) is developed and kept by F. Milano [28]. It is a Matlab toolbox for electric power system analysis. The main functions of this toolbox include: power flow analysis, optimal power flow analysis, small signal stability analysis, time domain simulation, etc. The power flow and time domain simulation functions are used in our simulation. We stretched the time domain simulation part to include the trajectory sensitivity calculation and do the MPC optimization. Figure 3.6 shows the overall flowchart of our simulation work. Data file contains the model and contingency information. It is the input to a power flow analysis. After that, time domain simulation is initialized by the power flow result and runs until the end of the prediction horizon of the first control sampling point. At iteration 1, voltage stability margin and its sensitivity with respect to controls are calculated. Trajectory sensitivity matrix calculation provides sensitivities with respect to control variables at the first control sampling point. Then the optimization program starts to run to get the control actions at each control step. After that, the first step of control actions is implemented and the control parameters of the system are updated in the control update step. Then time domain simulation for the next control sampling point is initialized. Time domain simulation runs until the next control sampling point. Iteration number is increased by 1. Then the program will check if the iteration number has reached the number of control steps. If yes, simulation ends. Otherwise, at the current control sampling point iter, repeat the sensitivity calculation, optimization, control update, etc.

The files related with the implementation of MPC based voltage control are listed in Table 4.1. This table contains 2 columns. The first column lists the function of the files. The second column contains the file names used in our MPC based voltage stabilization design.

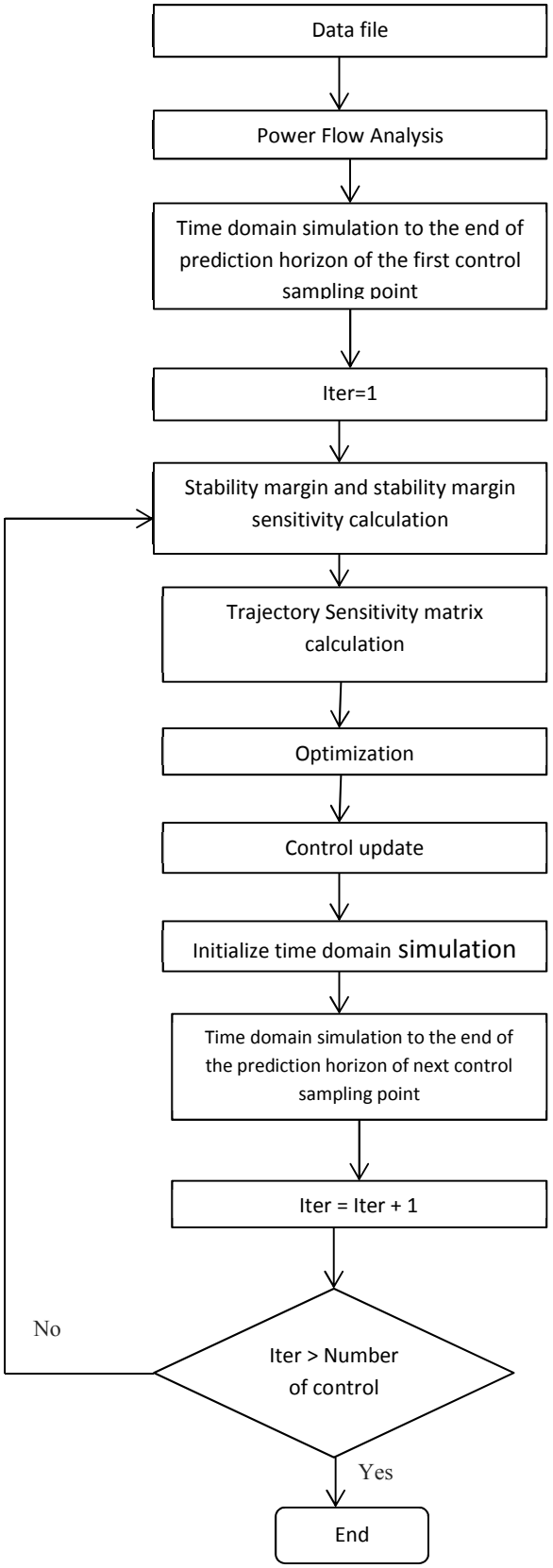

Figure 4.2 the flow chart of the MPC based control simulation

Table 4.1 The function and the associated file names in MPC implementation

Function	Files
Data File	Ethiopian Data.m
Power Flow Analysis	runpsat.m
Time Domain Simulation	runpsat.m
Sensitivity Calculation	SenAtCs.m
Optimization	MPCOpt.m
Initialize time domain simulation	InitializeTD.m
Main program	Ethiopian MPC.m,

4.3.2 Data file

The data file contains all the data used in power flow analysis and time domain simulation. It includes bus, transmission line, transformers, slack bus, PV bus, PQ bus, shunt, generator, load model, fault information, breaker, etc. Detailed information of these models can be finding in [39]. The following subsection introduces the data format used in the Data file.

4.3.2.1 Bus

Bus data is defined in Bus.con. Bus data format is in Table 4.2.

Table 4.2 Bus data format

Column	Description	unit
1	Bus number	int
2	Voltage base	kV
3	Voltage amplitude initial guess	p.u
4	Voltage phase initial guess	p.u
5	Area number	int
6	Region number	int

4.3.2.2 Transmission line and Transformer

Transmission line and transformer information are stored in Line.con. The data format is in Table 4.3.

Table 4.3 Line data format

Column	Description	Unit
1	From bus	int
2	To bus	int
3	Power rating	MVA
4	Voltage rating	kV
5	Frequency rating	Hz
6	Line length	km
7	Primary and secondary voltage ratio	kV/kV
8	Resistance	p.u
9	Reactance	p.u
10	not used	-
11	Fixed tap ratio	p.u/p.u
12	Fixed phase shift	deg
13	Current limit	p.u
14	Active power limit	p.u
15	Apparent power limit	p.u

Note: Column 6 only valid for transmission lines.Column 7 only valid for transformers.

4.3.2.3 Slack bus

Slack bus is a bus used to balance the real and reactive power in the system. It is a bus with fixed voltage magnitude and phase. The slack bus information is stored in SW.con. The data format is shown in Table 4.4.

Table 4.4 Slack bus data format

Column	Description	Unit
1	Bus number	int
2	Power rating	MVA
3	Voltage base	kV
4	Voltage magnitude	p.u
5	Reference angle	p.u
6	Maximum reactive power	int
7	Minimum reactive power	int
8	Maximum voltage	p.u
9	Minimum voltage	p.u
10	Active power guess	p.u
11	Loss participation coefficient	-

4.3.2.4 Active power-voltage (PV) bus

PV bus has fixed voltage magnitude and real power injection. The PV bus data information is stored in PV.con. The data format is shown in Table 4.5.

Table 4.5 PV bus data forma

Column	Description	Unit
1	Bus number	int
2	Power rating	MVA
3	Voltage base	kV
4	Active power	p.u
5	Voltage magnitude	p.u
6	Maximum reactive power	int
7	Minimum reactive power	int
8	Maximum voltage	p.u
9	Minimum voltage	p.u
10	Active power guess	p.u
11	Loss participation coefficient	-

4.3.2.5 Active and reactive power (PQ) load

PQ bus has a fixed real and reactive power injection. The PQ bus data information is stored in PQ.con. The data format is shown in Table 4.6.

Table 4.6 PQ bus data format

Column	Description	Unit
1	Bus number	int
2	Power rating	MVA
3	Voltage base	kV
4	Active power	p.u
5	Reactive power	p.u
6	Maximum voltage	p.u
7	Minimum voltage	p.u
8	Allow conversion to impedance	boolean

4.3.2.6 Shunt

Shunt data is stored in Shunt.con. The data format is shown in Table 4.7.

Table 4.7 Shunt data format

Column	Description	Unit
1	Bus number	int
2	Power rating	MVA
3	Voltage base	kV
4	Frequency rating	Hz
5	Conductance	p.u
6	Susceptance	p.u

4.3.2.7 Synchronous Machine

Synchronous machine data is stored in Syn.con. The data format is shown in Table 4.8.

Table 4.8 Synchronous machine data format

Column	Description	Unit
1	Bus number	int
2	Power rating	MVA
3	Voltage base	kV
4	Frequency rating	Hz
5	Machine model	-
6	Leakage reactance	p.u
7	Armature resistance	p.u
8	d-axis synchronous reactance	p.u
9	d-axis transient reactance	p.u
10	d-axis sub-transient reactance	p.u
11	d-axis open circuit transient time constant	s
12	d-axis open circuit sub-transient time constant	s
13	q-axis synchronous reactance	p.u
14	q-axis transient reactance	p.u
15	q-axis sub-transient reactance	p.u
16	q-axis open circuit transient time constant	s
17	q-axis open circuit sub-transient time constant	s
18	Mechanical starting time (2*inertia constant)	kWs/kVA
19	Damping coefficient	p.u
20	Speed feedback gain	gain
21	Active power feedback gain	gain
22	Active power ratio at node	[0,1]
23	Reactive power ratio at node	[0,1]
24	d-axis additional leakage time constant	s

4.3.2.8 Exponential Load Model

Exponential load model is introduced in chapter 2. The data related with this component is stored in Exload.con. The data format is shown in Table 4.9.

Table 4.9 Exponential recovery load data format

Column	Description	Unit
1	Bus number	int
2	Power rating	MVA
3	Active power voltage coefficient	kV
4	Active power frequency coefficient	Hz
5	Real power time constant	s
6	Reactive power time constant	s
7	Static real power exponent	-
8	Dynamic real power exponent	-
9	Static reactive power exponent	-
10	Dynamic reactive power exponent	-

4.3.2.9 Fault

Table 4.10 shows data for a three-phase fault. The data is contained in Fault.con.

Table 4.10 Fault data format

Column	Description	Unit
1	Bus number	int
2	Power rating	MVA
3	Voltage base	kV
4	Frequency rating	Hz
5	Fault time	p.u
6	Clearance time	p.u
7	Fault resistance	p.u
8	Fault reactance	p.u

4.3.3 Power flow

The power flow problem is formulated as the solution of a nonlinear set of equations as follows:

$$\dot{x} = 0 = f(x, y) \tag{4.12}$$

$$0 = g(x, y) \tag{4.13}$$

where y are the algebraic variables i.e. voltage magnitudes and phase angles. x are the state variables, such as generator electrical rotor angle, rotor speed, etc. Newton-Raphson method is used to solve the power flow problem. At each step, the Jacobian matrix of Equation (4.12) is updated and linear equation (4.13) is solved until Δx^i and Δy^i is less than the tolerance or the iteration number reaches maximum (the latter case indicates that power flow cannot converge).

$$\begin{bmatrix} \Delta x^i \\ \Delta y^i \end{bmatrix} = -\begin{bmatrix} F_x^i & -F_y^i \\ G_x^i & G_y^i \end{bmatrix}^{-1} \begin{bmatrix} f^i \\ g^i \end{bmatrix}, \tag{4.14}$$

$$\begin{bmatrix} x^{i+1} \\ y^{i+1} \end{bmatrix} = \begin{bmatrix} x^i \\ y^i \end{bmatrix} + \begin{bmatrix} \Delta x^i \\ \Delta y^i \end{bmatrix} \tag{4.15}$$

4.3.4 Time domain simulation

Time domain simulation is a commonly used way to study dynamic behavior of power systems. Consider the DAE model.

$$\dot{x} = f(x, y) \tag{4.16}$$

$$0 = g(x, y) \tag{4.17}$$

Trapezoidal approach is used to approximate Equation (4.16) with a set of algebraic difference equations coupled to the original algebraic Equation (4.17). The evolution of the states x, and y from time instant t_i to the next time instant t_{i+1} can be described as

$$x^{i+1} = x^i + \frac{\eta}{2}(f(x^{i+1}, y^{i+1}) + f(x^i, y^i)) \tag{4.18}$$

$$0 = g(x^i, y^i) \tag{4.19}$$

where superscript i is the time instant t_i, i + 1 is the time instant t_{i+1} and $\eta = t_{i+1} - t_i$ is the integration time step. Rearrange Equation (4.18) and Equation (4.19) as follows:

$$F = \begin{bmatrix} \frac{\eta}{2} f(x^{i+1}, y^{i+1}) - x^{i+1} + \frac{\eta}{2} f(x^i, y^i) + x^i \\ g(x^{i+1}, y^{i+1}) \end{bmatrix} = 0 \tag{4.20}$$

Equation (4.20) is a set of implicit nonlinear algebraic equations. The Newton iterative technique is commonly used to solve for x^{i+1} and y^{i+1}, given x^i and y^i

$$\begin{bmatrix} x^{i+1} \\ y^{i+1} \end{bmatrix} = \begin{bmatrix} x^i \\ y^i \end{bmatrix} - F_x^{-1} F \tag{4.21}$$

where, F_x is the Jacobian of F with respect to x, y.

$$F_x = \begin{bmatrix} \frac{\eta}{2} f_x - I \frac{\eta}{2} f_y \\ g_x \qquad g_y \end{bmatrix} \tag{4.22}$$

4.3.5 Trajectory Sensitivity

The basic concept of trajectory sensitivity has been introduced in in previous section. Here, we introduce the numerical realization of trajectory sensitivities. Differentiating Equations (4.16) and (4.17) with respect to the initial conditions x_0 results in the DAEs of trajectory sensitivities

$$\dot{x}_{x_0} = f_x x_{x_0} + f_y y_{x_0} \tag{4.23}$$

$$0 = g_x x_{x_0} + g_y y_{x_0} \tag{4.24}$$

The trajectory sensitivity can be approximated by trapezoidal integration as follows:

$$x_{x_0}^{i+1} = x_{x_0}^i + \frac{\eta}{2}(f_x^i x_{x_0}^i + f_y^i y_{x_0}^i + f_x^{i+1} x_{x_0}^{i+1} + \overline{f}_y^{i+1} y_{x_0}^{i+1}) \tag{4.25}$$

$$0 = g_x^{i+1} x_{x_0}^{i+1} + g_y^{i+1} y_{x_0}^{i+1} \tag{4.26}$$

Rearranging the above equation results in

$$\begin{bmatrix} \frac{\eta}{2} f_x^{i+1} - I\frac{\eta}{2} f_y^{i+1} \\ g_x^{i+1} \quad g_y^{i+1} \end{bmatrix} \begin{bmatrix} x_{x_0}^{i+1} \\ y_{x_0}^{i+1} \end{bmatrix} = \begin{bmatrix} -\frac{\eta}{2}(f_x^i x_{x_0}^i, f_y^i y_{x_0}^i) - x_{x_0}^i \\ 0 \end{bmatrix} \tag{4.27}$$

Therefore, the sensitivity matrix $\begin{bmatrix} x_{x_0}^{i+1} \\ y_{x_0}^{i+1} \end{bmatrix}$ can be obtained as a solution of a linear matrix equation. Notice that the coefficient matrix of Equation (4.11) is exactly the same as Jacobian matrix F_x (in Equation (4.8)) in solving for x_{i+1} and y_{i+1} in time domain simulation.

4.3.6 Voltage Stability Margin

For the security constrained voltage control design, voltage stability margin and sensitivities of voltage stability margin with respect to control need to be calculated at each iteration. The mathematical formulation is in Chapter 3 Section 3.2.3.

4.3.7 Optimization

The optimization problem solved in each sampling point of MPC is actually a quadratic programming as follows:

Minimize

$$x^T Q x + f' x$$

Subject to

$$Ax <= B$$

$$l \le x \le u$$

Where Q and f' are parameters of the cost function, A, B are parameters defining the inequality constraints and l,u are upper and lower limits of variable x.

4.3.8 Initialize time domain simulation

Time domain simulation needs a starting point, i.e. x_0 and y_0. When time domain simulation starts from normal condition, a power flow result is used to initialize it. However, when it starts from any control sampling point, a snapshot of the system is used

to initialize the time domain simulation. Therefore, this step initializes a time domain simulation with a system snapshot and necessary parameters.

4.3.9 Main program

Main program realizes the function shown in Figure 4.2 by calling different modules introduced above. The output of a main program is the control matrix as well as system behavior with the designed controls.

CHAPTER 5. Simulation Result and Discussion

5.1 Overview

The suggested method is illustrated using the modified Ethiopian 400kV and 230kV 30-bus system. The exponential recovery load model is used. The parameters of the load model are as following:

$T_p = T_q = 30$, $\alpha_s = 0$, $\alpha_t = 1$, $\beta_s = 0$, $\beta_t = 4.5$.

The parameters in MPC optimization are determined based on the following considerations. Any voltage instability following a contingency must be stabilized in certain time duration (typically the time in which voltage will decrease by 15%). This is the prediction horizon T_p. The control should be exercised on a time horizon T_c, which is shorter than the prediction horizon, typically the time in which voltage will decrease by 10% (if no control is applied). A discrete-time control must be applied within this duration T_c at a sample-rate high enough to adequately react to the changing voltage trajectory, as well as to allow accurate enough predictions of the voltage trajectory based on the linearization of the trajectory-sensitivity. This dictates the sampling duration T_s. The number of sampling point N is then determined as the ratio of T_c and the sampling duration T_s. The voltage control means in the test cases include SVCs, LTCs, and load shedding. To avoid over-voltage problems, the maximum amount of the controls is limited at each sampling point. For SVCs, the maximum control amount is 0.1p.u. The maximum number of load tap changer steps is 3. And the maximum load shedding at one sampling point is 10%. The step size of LTCs is 0.006p.u. The step size of load shedding is 5%.

5.2 Modified Ethiopian 6-Generator 30-Bus Test System

5.2.1 System description

The proposed method is illustrated using a modified Ethiopian 30-bus system as shown in Figure 5.1. There are totally 32 buses and 6 generators. Two transformer banks with load tap changers are added between bus 8 and bus 31, bus 4 and bus 32. A fourth-order generator model is used. The exception is that a third-order model is used for the generator at bus 30 that does not include the d-axis transient voltage as part of the state space. In addition, all generators excluding those at bus 27 have automatic voltage

regulators (AVRs), which are represented by fourth-order models. There are around 14 loads are consider which are represented by the exponential recovery dynamic models with two dimension. The total dimension of the state space is 72.The parameters of the load model are $T_p = T_q = 30$; $\alpha_s = 0$; $\alpha_t = 1$; $\beta_s = 0$; $\beta_t = 4.5$. The control variables are as follows:

- SVCs at buses 2, 6, 17, and 19;
- Load tap changers at the transformer banks between bus 8 and bus 31, bus 4 and bus 32;
- Load shedding at bus 15 and bus 16.

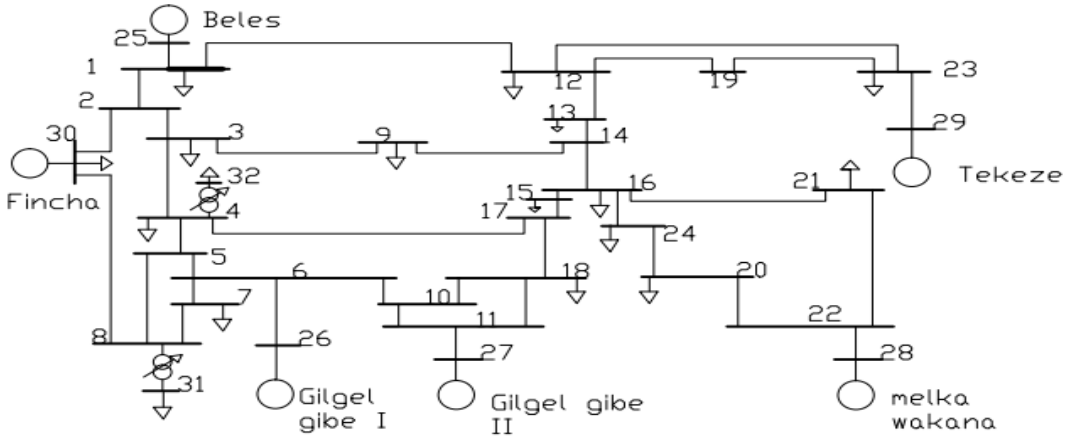

Figure 5.1 Modified Ethiopian 230 kV and 400kV 30-bus network system.

Load shedding is an emergency voltage control action. A higher cost weight should be used to make sure that load shedding is trigged only when other control actions are not sufficient. To avoid over-voltage problems, the maximum amount of the controls is limited at each sampling point. For SVCs, the maximum control amount is 0.1p.u. The maximum number of load tap changer steps is 3 and the maximum load shedding at one sampling point is 10%. The step size of LTCs is 0.006p.u. The step size of load shedding is 5%.

5.2.2 Fault scenario

As we have mentioned in the above sub section we have many fault scenarios in power system but we obligate to consider only one type of fault because the process become very complex and difficult to handle. Therefore, the contingency considered here is a

three-phase-to-ground fault at bus 21 at t = 1.0 second, which is cleared at t = 1.2 seconds by the tripping of the transmission line between bus 21 and bus 22. Voltage behavior of the modified Ethiopian system is shown in Figure. 5.2. From t = 0 second to t = 1.0 second, voltages are constant representing that they are in steady state. At time t = 1.0 second, voltages drop dramatically when the fault occurs. After the fault is cleared at 1.2 seconds, the voltages recover greatly whereas some oscillations follow but this oscillation is very dangerous for the material involved in the system. After seconds later, the oscillations are damped out, but the voltages start to decline slowly because of the exponential recovery of the loads. Around 1 minutes later, the voltages collapse.

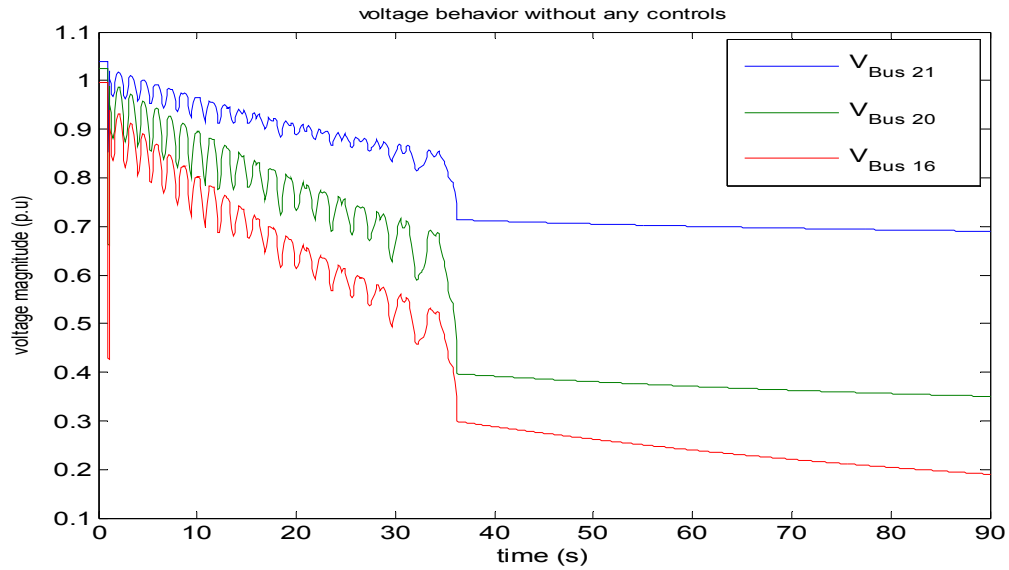

Figure 5.2 Voltage behavior of the 6-generator 32-bus test system without MPC control

5.2.3 Simulation result with coordinate control

In this test case too, there are three types of voltage control options. They are LTCs, SVCs and load shedding. This subsection studies the effect of coordinate control on the restoration of the voltage behavior. There are mentioned on Table 5.1, which locate in the network. The upper limit of these SVCs, LTCs and load shedding is 0.3p.u, 3p.u, 10p.u respectively. The control strategy is to switch all the available coordinate controls of SVCs at 20 seconds. The voltage behavior is presented in Figure 5.3. From this figure, we find that though all the coordinate controls are put into use, the voltage cannot be stabilized following the contingency as well as at the initial there is an overshot and also

it is dangerous for the system and instrument that involve in electric power system. Therefore, we need a special control mechanism to solve the drawback of coordinate control voltage stabilization that mentioned in the above. So the model predictive control can solve the weakness of the coordinate control mechanism.

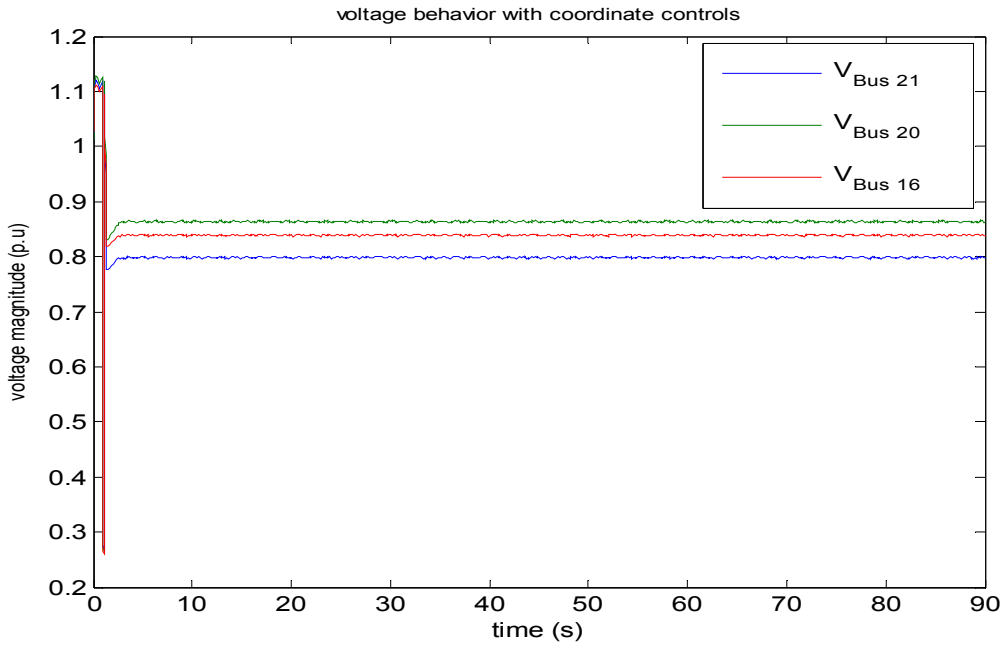

Figure 5.3 Voltage behavior of the modified Ethiopian system with coordinate control

Table 5.1 The control strategy for the 6-generator 32-bus test system

Time(second)	20	35	50	65	75
SVC at bus 2 (p.u.)	0	0	0	0	0
SVC at bus 6 (p.u.)	0	0.0215	0	0	0
SVC at bus 17 (p.u.)	0.0065	0.1	0.1	0.094	0
SVC at bus 19 (p.u.)	0	0	0.013	0.093	0
LTC between buses 8 and 31 (steps)	3	3	3	3	0
LTC between buses 4 and bus 32 (steps)	3	3	3	3	0
Load shedding at bus 15 (%)	10	10	10	5	5
Load shedding at bus 16 (%)	10	10	0	0	0

5.2.4 Simulation result with model predictive control

In this example, we have chosen prediction horizon T_p to be 90 seconds (the time in which voltage drops by nearly 12% at bus 21). T_c has been chosen to be 75 seconds. We found that sample duration of T_s = 15 seconds works well for this example, and so we have the number of control steps: $N = \frac{T_c}{T_s} = \frac{75}{15} = 5$. The control action determined by the MPC based algorithm starts around 20 seconds to recover voltage. The system response with MPC in place is shown in Figure. 5.4. With the MPC implemented, the voltages are stabilized at a value between [0.95, 1.05]p.u and it is stable in the system and also we have guaranteed to the safety of electric equipment from damage at the instant of the fault occurred . The corresponding control strategy is shown in Table 5.1. It can be famous in the table that the load tap changers are applied to the maximum allowed at each sampling point. Load shedding is also used to stabilize the system. The table shows a coordinated control strategy among load tap changers, static var compensators and load shedding is utilized for voltage stabilization with a certain stability margin. As shown in simulations, MPC is applied after a fault has occurred, and it is not required that MPC be used before the occurrence of a fault. Also since MPC is applied after a fault, the initial condition is arbitrary in all our simulations, i.e., the MPC-based control is successful autonomously of the initial conditions.

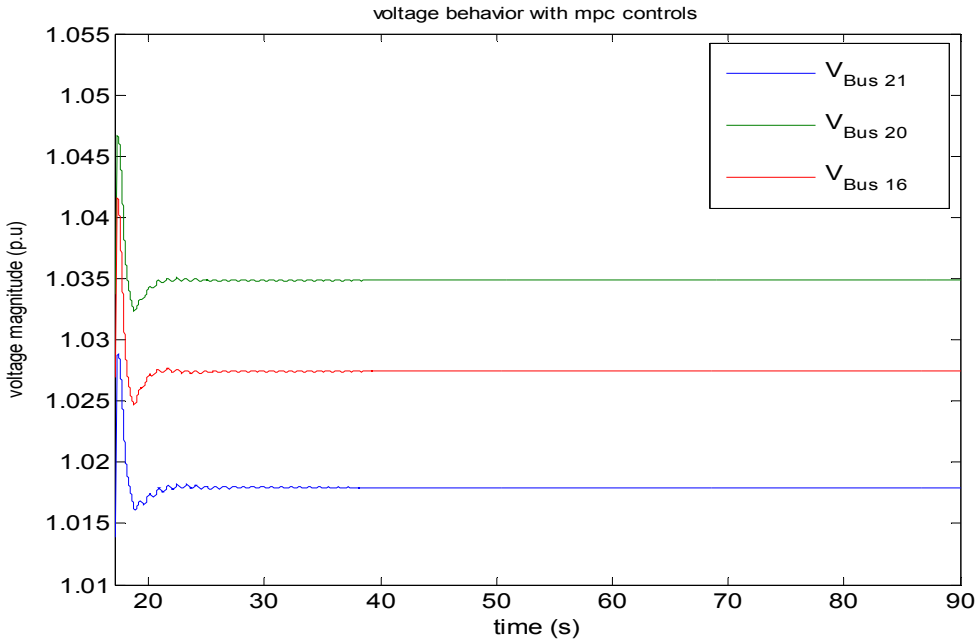

Figure 5.4 Voltage behavior of the modified Ethiopian system with MPC-based coordinated voltage control

5.3 Implementation Issues

Figure 1.3 presents a general architecture for the carrying out a real time SPS. The functional structure of implementing the MPC based coordinated voltage control proposed above is shown in Figure 5.5. Line flow measurements, bus voltage information, and switch status measured by phase measurement units (PMUs) and collected by Phasor Data Concentrators (PDCs) are sent to a control center through communication channels. These measurements plus a network model are used by the state estimator (SE) for filtering out the noise and estimating the auxiliary (also known as static state) variables. The results from the state estimator are used for power flow analysis. A power flow solution is then used by an on-line dynamic security assessment program to initialize the state variables of the dynamic models. Further, it uses system models and disturbance information to perform the contingency analysis to evaluate the security margin of the power system. If a contingency is identified where the system will become unstable, MPC based computation gets caused at the time an identified critical contingency occurs. A final step is to implement the computed control to improve the

security of the power system. The steps of the MPC computation in the k^{th} iteration include:

- Estimate static variables $y(t_k)$ such as voltage magnitudes and angles at time t_k as well as the dynamic variables $x(t_k)$ such as generator angles, velocities and real and reactive load recovery. The values of the static variables are provided by the state-estimator. As far as the dynamic variables are concerned, they can be classified into short-term dynamic variables (such as generator angles and velocities) and long-term dynamic variables (such as real and reactive load recovery). The values of the long-term dynamic variables can be directly measured and hence are known, whereas the short-term dynamic variables are in quasi steady-state (QSS) with respect to the long-term voltage/frequency stability

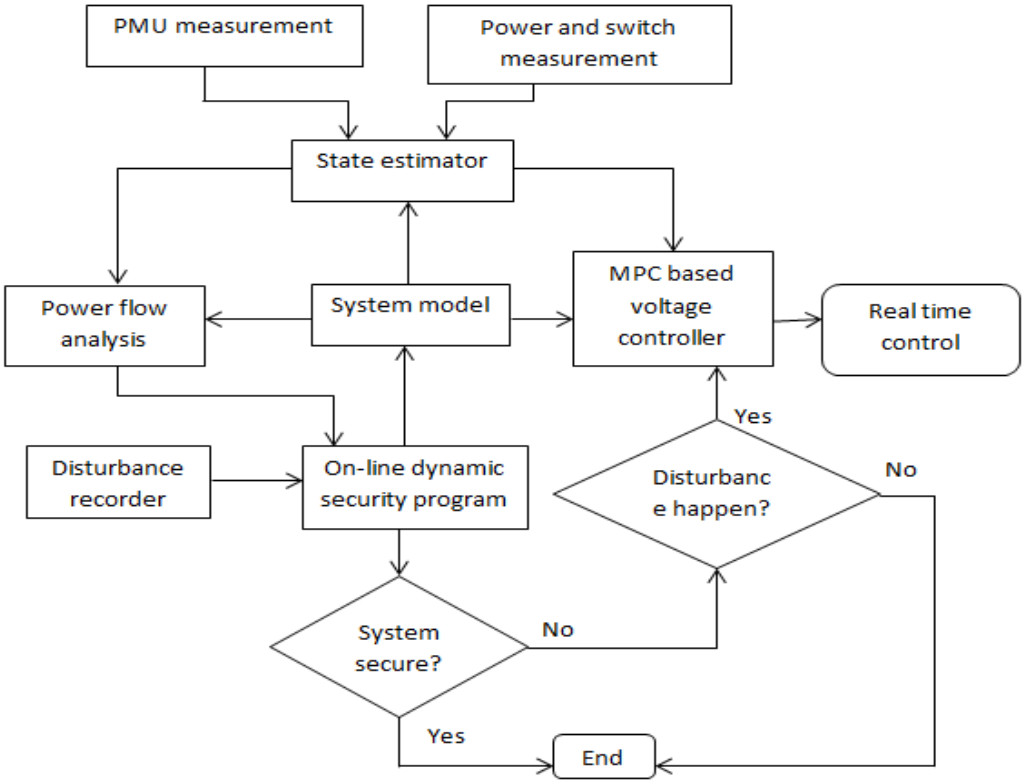

Figure 5.5 Structure of implementing a MPC based Voltage stabilization.

phenomenon investigated in this paper. Thus the values of the short-term dynamic variables can be obtained by solving an equilibrium equation of the form:

$$0(=\dot{x}_s) = f_s(x_s, x_l, y, u), \tag{5.1}$$

Where x_s is the short-term dynamic variable vector (to be computed by solving (5.1)), x_l is long term dynamic variable vector (which is measured and hence known), y is the static variable vector (which is provided by the state-estimator and hence known), and u is the input variable vector (which is of course known). Then in equation (5.1), the number of unknowns (dimension of x_s) is the same as the number of equations (dimension of f_s), and so the short-term dynamic variables can be computed by solving (5.1).

- Run time-domain simulation to compute the system trajectory given the current state.
- Obtain trajectory sensitivities of voltage with respect to the control variables as a result of the time-domain simulation performed in the previous step.
- Obtain voltage stability margin with respect to the control variables based on a continuation power flow program.
- Solve the quadratic programming optimization problem and implement the first step of the control.

For all the work that has been done in this chapter, all the required algorithms have been developed in Matlab. For the test case in section 3.5, the total computation time is around 10 minutes. The 95 percent of the computation time is used for time domain simulation. For a potential practical application of the proposed approach, a commercial grade programming should be used to improve the computation performance (time, numerical accuracy, etc.). The proposed approach is model based, and so it requires the availability of accurate models. The models are partially already available and the others are being modelled by us used for state-estimation and dynamic security assessment. For those power system applications where accurate models are not available, there is no choice but to continue using the rules based predefined SPSs. We also realize that the measurements can be noisy as well as delayed. The "MPC based voltage controller" block however does not directly deal with the measurements. These are input to the "State Estimator" or "Dynamic Security Assessment" blocks, and these blocks are designed to cope with noisy/delayed measurements.

CHAPTER 6. Conclusion and Future Work

6.1 Conclusion

This thesis states a coordinated voltage control strategy for voltage stability following disturbances in Ethiopia high voltage power network system. The design is based on system protection scheme on MPC method with a decreasing control horizon. Trajectory sensitivity technic is used to measure the effect of controls on the voltage improvement. The iterative optimization procedure of MPC helps confirm that errors introduced due to trajectory sensitivity linearization and any model inaccuracies are minimized. The coordination of static var compensators, under load tap changers and load shedding is attained by solving a quadratic mixed integer optimization formulation.

The 30-bus Ethiopian system test case shows that the proposed MPC-based coordinated control strategy can effectively attain the desired system performance.

The model prediction control based coordinated control for voltage stabilization and security proposed in this thesis is anticipated to be applicable for industrial-size systems. The control computation at each control step in trajectory sensitivity needs (i) estimation of static and dynamic variables, (ii) time-domain simulation to predict system trajectory starting from lately estimated state under the controls applied in the past steps, (iii) trajectory-sensitivity computation, (iv) quadratic mixed-integer programming solution. The most time-consuming component, dominating the other components, is time-domain simulation. Currently there already exist on a traditional system protection scheme and propose online real time system protection scheme based on model predictive control. It runs stability study for single contingencies for a 30 bus system based on a time domain simulation and we can get what we propose (i.e. between 0.95 and 1.05 p.u). We believe therefore that it should be possible to design controls based on the proposed method for on-line real-time system protection against a single contingency.

6.2 Directions of future research

Based on the proposed research work in the thesis, future research might be done in a variety of directions. Potential research focus could include the following areas:

- **Expose our power network system to research.** There is no well-organized power network and data in the Ethiopia power system. This make it hides for different researcher and done different research on it to modernize the utility of the organization to give the costumer.
- **Dynamic state estimation**. Existing state estimation is based on static analysis. The inputs to a state estimator are status of circuit breakers, voltage magnitudes, real and reactive power consumption of loads, transmission line and transformer flow and generator outputs. The outputs include all real and reactive power consumption of loads, generator real power outputs and voltage magnitudes of generator buses. In the future, we need focus on the dynamic state estimation to solve the problem in overall Ethiopian power network system.
- **Time delay issue**. To implement the MPC based control strategy, we must send the signal to substations. This communication involves time delay. In the future, we need investigate the effect of time delay on the effectiveness of MPC based control schemes.
- **Robustness of method**. We studied the robustness of the MPC based control schemes by time domain simulation. Alternative direction is to develop a systematic way to do the robustness study like optimal power flow method, direct method integration etc. in our country power system.

Reference

[1] Crow, M., Infrastructure roots," *evolution of electric power in the United States*", *Power and Energy Magazine, IEEE, 1(2):pp.20-21, 2003.*

[2] Hein, J. T.,"*An essential industry at the crossroad: deregulation, restructuring and a new model for the United States' bulk power system*", Master's thesis, University of Colorado at Denver,2003.

[3] Available [online] www.eepco.gov.et/**corporationhistory**.php

[4] Liacco, T. E. D.,"*The adaptive reliability control system*",*IEEE Transactions on Power Apparatus and Systems, PAS-86(5):pp.517-531,1967.*

[5] Fouad, A. A., Aboytes, F., Carvalho, V., Corey, S., Dhir, K., and Vieera, R., "*Dynamic security assessment practices in North America*", *IEEE Transactions on Power Systems, 3(3):pp.1310-1321, 1988.*

[6] Debs, A.S.,"*Modern Power Systems Control and Operation*", Kluwer Academic, Maryland,1988.

[7] Rahimi, F. A., Lauby, M. G., Wrubel, J. N., and Lee, K. L., "*Evaluation of the transient energy function method for on-line dynamic security analysis*", *IEEE Transactions on Power Systems, 8(2):pp.497-507, 1993.*

[8] Anthony, N. M., Fouad, A. A., and Vittal, V.,"*Power system transient stability using individual machine energy functions*",*IEEE Transactions on Circuits and Systems, 30:pp.266-276,1983.*

[9] Kundur, P., Paserba, and J., Ajjarapu, V., Andersson, G., Bose, A., and etc., "*Deffinition and classification of power system stability*", *IEEE Transactions on Power Systems, 15:pp.1387-1401, 2004.*

[10] Kundur, P.,"*Power System Stability and Control*", McGraw Hill, New York,1994.

[11] Morison, G. K., Gao, B., and Kundur, P.,"*Voltage stability analysis using static and dynamic approaches*", *IEEE Transactions on Power Systems, 8:pp.1159-1171, 1993.*

[12] CIGRE Task Force 38.02.14 Rep.,"*Analysis and modeling needs of power system under major frequency disturbances*",1999.

[13] Doudna, J. H.,"*Application and implementation of fast valving and generator tripping schemes at Gerald Gentleman station*",*IEEE Transactions on Power Systems, 3(3):pp.1155-1166,1988.*

[14] Karlsson.D.and Waymel.X.,"*System protection schemes in power networks*", *Technical report, CIGRE Task Force, 2001.*

[15] Liu, H. Jin, L. McCalley, J. D., Kumar, R., and Ajjarapu, V.," *Linear complexity search algorithm to locate shunt and series compensation for enhancing voltage stability*", *In Proceedings of the 37th Annual North American Power Symposium, pp. 344-350,2005.*

[16] Bergen.A. and Vittal, V.,"*Power system analysis*", Prentice Hall, Inc,1999.

[17] Pai, M. A.,"*Power system dynamics and stability*", Prentice Hall, Inc.

[18] IEEE Committee Report (1981),"*Excitation system models for power system stability studies*", *IEEE Transactions on Power Apparatus and Systems, PAS-100(5):pp.494-509,1998.*

[19] Karlsson, D. and Hill, D.," *Modeling and identification of nonlinear dynamic loads in power systems*", *IEEE Transactions on Power Systems, 9(1):pp.157-166, 1994.*

[20] Rawlings, J.,"*Tutorial overview of model predictive control*", *IEEE Control Systems Magazine, 20(3):pp.38-52,2000.*

[21] Larsson, M., Hill, D. J., and Olsson, G.," *Emergency voltage control using search and predictive control*", *International Journal of Power and Energy Systems, 24(2):pp.121-130, 2002.*

[22] Larsson, M. and Karlsson, D.," *Coordinated system protection scheme against voltage collapse using heuristic search and predictive control*", *IEEE Transactions on Power Systems, 18(3):pp.1001-1006, 2003.*

[23] Wen, J. Y. and Wu, Q. H.,"*Optimal coordinated voltage control for power system voltage stability*", *IEEE Transactions on Power Systems, 19(2):pp.1115-1122, 2004.*

[24] Zima, M. and Andersson, G.," *Model predictive control employing trajectory sensitivities for power systems applications*", *In Proceedings of the 44-nd IEEE Conference on Decision and Control, pp.4452-4456*, Seville, Spain,2005.

[25] Hiskens, I. A. and Gong, B.,"*MPC-based load shedding for voltage stability enhancement*", *In 44th IEEE Conference on Decision and Control, pp. 4463-4468,* Seville,Spain,2005.

[26] Atic, N., Rerkpreedapong, D., Hasanovic, A., and Feliachi, A.," *NERC compliant decentralized load frequency control design using model predictive control*", *In 2003 IEEE Power Engineering Society General Meeting, pp. 554-559, Toronto, Canada,2003.*

[27] Milano.F.,"*An open source power system analysis toolbox*", *IEEE Transactions on Power Systems, 20(3): pp.1199-1206, 2005.*

[28] Khalil, H. K.," *Nonlinear System (Third Edition)*", Prentice Hall, New Jeasey, 2002.

[29] El-Kady, M. A., Bell, B. D., Carvalho, V. F., Burchett, R., Happ, H. H., and Vierath, D. R.," *Assessment of real - time optimal voltage control*", *IEEE Transactions on Power Systems, PWRS-1(2):,pp.98-105,1986.*

[30] Liu, C. C. and Tomsovic, K.,"*An expert system assisting decision-making*", *IEEE Transactions on Power Systems, PWRS-1(3): pp.195-201, 1986.*

[31] Wagner, W. R., Keyhani, A., Hao, S., and Wong, T. C.," *A rule based approach to decentralized voltage control*", *IEEE Transactions on Power Systems, 5(2):pp.643-651, 1990.*

[32] Matsuda, S., Ogi, H., Nishimura, K., Okataku, Y., and Tamura, S.," *Power system voltage control by distributed expert systems*", *IEEE Transactions on Power Systems, 37(3):pp.236-240, 1990.*

[33] Godart, T. F. and Puttgen, H. B.," *A reactive path concept applied within a voltage control expert system*", *IEEE Transactions on Power Systems, 6(2):pp.787-793.*

[34] Vu, H., Pruvot, P., Launay, C., and Harmand, Y. (1996),"*An improved voltage control on large-scale power system*", *IEEE Transactions on Power Systems, 11(3):pp.1295-1303, 1991.*

[35] Corsi, S., Pozzi, M., Sabelli, C., and Serrani, A.,"*The coordinated automatic voltage control of the Italian transmission grid-part II: control apparatuses and field performance of the consolidated hierarchical system*", *IEEE Transactions on Power Systems, 19(4):pp.1733-1741, 2004b.*

[36] Corsi, S., Pozzi, M., Sabelli, C., and Serrani, A.,"*The coordinated automatic voltage control of the Italian transmission grid-part I: reasons of the choice and overview of the consolidated hierarchical system*", *IEEE Transactions on Power Systems, 19(4):pp.1723-1732, 2004a.*

[37] Sancha, J. L., Fernandez, J. L., Cortes, A., and Abarca, J. T.," *Secondary voltage control: analysis, solutions and simulation results for the Spanish transmission system*", *IEEE Transactions on Power Systems, 11(2):pp.630-638, 1996.*

[38] Hecke, J. V., Janssens, N., Deuse, J., and Promel, F.," *Coordinated voltage control experience in Belgium*", *Technical report, CIGRE Task Force pp.38-111, 2000.*

[39] Taranto, G., Martins, N., Martins, A. C. B., Falcao, D. M., and Santos, M. G. D.," *Benefits of applying secondary voltage control scheme to the Brazilian system*", *In Proceedings of Power Engineering Society Summer Meeting, pp .937-942,2000.*

[40] Marques, A. B., Taranto, G. N., and Falcao, D. M.,"*A knowledge-based system for supervision and control of regional voltage profile and security*", *IEEE Transactions on Power Systems, 20(1):pp.400-407, 2005.*

[41] Paserba, J., Leonard, D., Miller, N., Naumann, S., Lauby, M., and Sener, F., "*Coordination of a distribution level continuously controlled compensation device with existing substation equipment for long term var management*", *IEEE Transactions on Power Delivery, 20(2):pp.1034-1040, 1994.*

[42] Park, J. Y., Nam, S. R., and Park, J. K.,"*Control of a ULTC considering the dispatch schedule of capacitors in a distribution system*", *IEEE Transactions on Power Systems, 22(2):pp.755-761,2007.*

[43] Kim, G. and Lee, K.,"*Coordination control of ULTC transformer and STATCOM based on an artificial neural network*", *IEEE Transactions on Power Systems, 2(2):pp.580-586, 2005.*

[44] Larsson, M., Hill, D. J., and Olsson, G.," *Emergency voltage control using search and predictive control*", *International Journal of Power and Energy Systems, 24(2):pp.121-130,2002.*

[45] Larsson, M. and Karlsson, D.,"*Coordinated system protection scheme against voltage collapse using heuristic search and predictive control*", *IEEE Transactions on Power Systems, 18(3):pp.1001-1006,2003.*

[46] IEEE Committee Report ,"*Computer representation of excitation systems*", *IEEE Transactions on Power Apparatus and Systems, PAS-87(6):pp.1460-1464,1968.*

[47] Ajjarapu, V. and Christy, C.,"*The continuation power flow: a tool for steady state voltage stability analysis*", *IEEE Transactions on Power Systems, 7(1):pp.416-423,* 1992.

[48] Smed, T.," *Feasible eigenvalue sensitivity for large power systems*", *IEEE Transactions on Power systems, 8(2):pp.555-563,* 1993.

Appendix

Ethiopian Data.m

```
Bus.con = [ ...
   1  400  1.03  0.3256  1  1;
   2  230  1.02  0.1567  1  1;
   3  230  1.01  0.2543  1  1;
   4  230  1.01  0.2476  1  1;
   5  230  1.03  0.3123  1  1;
   6  230  1.02  0.1765  1  1;
   7  230  1.01  0.2456  1  1;
   8  230  1.01  0.1125  1  1;
   9  230  0.9976  0.2546  1  1;
  10  230  0.9879  0.1423  1  1;
  11  400  0.9987  0.2347  1  1;
  12  230  0.9543  0.3211  1  1;
  13  230  0.9899  0.2543  1  1;
  14  230  1.02  0.2765  1  1;
  15  230  1.03  0.2134  1  1;
  16  230  1.01  0.3215  1  1;
  17  230  1.03  0.2542  1  1;
  18  230  1.02  0.3425  1  1;
  19  230  1.03  0.3245  1  1;
  20  230  1.02  0.2134  1  1;
  21  230  1.01  0.1765  1  1;
  22  230  0.9989  0.2435  1  1;
  23  230  0.9981  0.2489  1  1;
  24  230  1.02  0.3654  1  1;
  25  15   1.01  0.2413  1  1;
  26  13.8 1.03  0.3001  1  1;
  27  15   1.01  0.2101  1  1;
  28  13.8 1.02  0.3105  1  1;
  29  13.8 1.01  0.2590  1  1;
  30  13.8 0.9987 0.1543  1  1;
  ];
Line.con = [ ...
   1    2  115 400 50 0 0  0.0035  0.0411  0.6987  0  0 1    0    0  1;
   25   1  115 15  50 0 0  0.0010  0.0250  0.7500  0  0 1    0    0  1;
   1   12  115 400 50 0 0  0.0013  0.0151  0.2572  0  0 1    0    0  1;
   30   2  130 13.8 50 0 0 0.0070  0.0086  0.1460  0  0 1    0    0  1;
   2    3  130 230 50 0 0  0.0013  0.0213  0.2214  0  0 1    0    0  1;
   3    9  115 230 50 0 0  0.0011  0.0133  0.2138  0  0 1    0    0  1;
   3    4  130 230 50 0 0  0.0008  0.0128  0.1342  0  0 1    0    0  1;
   4   17  130 230 50 0 0  0.0008  0.0129  0.1382  0  0 1    0    0  1;
   4   5   130 230 50 0 0  0.0002  0.0026  0.0434  0  0 1    0    0  1;
   5   8   130 230 50 0 0  0.0008  0.0112  0.1476  0  0 1    0    0  1;
   5   6   61 230 50 0 0  0.0006  0.0092  0.1130  0  0 1    0    0  1;
```

```
   6   10  95 230 50 0 0  0.0007  0.0082  0.1389  0  0 1    0    0  1;
   26   6  61 13.8 50 0 0 0.0004  0.0046 0.0780   0  0 1    0    0  1;
   6   7   61 230 50 0 0  0.0023  0.00363 0.3804  0  0 1    0    0  1;
   7   8   61 230 50 0 0  0.0010  0.0250  1.2000  0  0 1    0    0  1;
   30   8  130 13.8 50 0 0 0.0004  0.0043  0.0729  0  0 1    0    0  1;
  10   11  95 230 50 0 0  0.0004  0.0043  0.0729  0  0 1    0    0  1;
  10   18  95 230 50 0 0  0.0009  0.0101  0.1723  0  0 1    0    0  1;
  27   11  95 15  50 0 0  0.0018  0.0217  0.3660  0  0 1    0    0  1;
  11   18  95 400 50 0 0  0.0009  0.0094  0.1710  0  0 1    0    0  1;
  18   17  95 230 50 0 0  0.0007  0.0089  0.1342  0  0 1    0    0  1;
  17   15  95 230 50 0 0  0.0016  0.0195  0.3040  0  0 1    0    0  1;
  15   16  95 230 50 0 0  0.0008  0.0135  0.2548  0  0 1    0    0  1;
  16   24  95 230 50 0 0  0.0003  0.0059  0.0680  0  0 1    0    0  1;
  16   21  150 230 50 0 0  0.0007  0.0082  0.1319  0  0 1    0    0  1;
  16   14  95 230 50 0 0  0.0013  0.0173  0.3216  0  0 1    0    0  1;
  14   13  95 230 50 0 0  0.0008  0.0140  0.2565  0  0 1    0    0  1;
  13   12  100 230 50 0 0  0.0006  0.0096  0.1846  0  0 1    0    0  1;
  12   23  100 230 50 0 0  0.0022  0.0350  0.3610  0  0 1    0    0  1;
  12   19  100 230 50 0 0  0.0032  0.0323  0.5130  0  0 1    0    0  1;
  19   23  100 230 50 0 0  0.0014  0.0147  0.2396  0  0 1    0    0  1;
  29   23  100 13.8 50 0 0 0.0043 0.0474  0.7802   0  0 1    0    0  1;
  21   22  150 230 50 0 0  0.0057  0.0625  1.0290  0  0 1    0    0  1;
  22   20  150 230 50 0 0  0.0014  0.0151  0.2490  0  0 1    0    0  1;
  28   22  150 13.8 50 0 0 0.0016 0.0435  0.6578   0  0 1    0    0  1;
  20   24  150 230 50 0 0  0.0009  0.0200  0.3456  0  0 1    0    0  1;
  9    14  130 230 50 0 0  0.0007  0.0235  0.6532  0  0 1    0    0  1;
  ];
Breaker.con = [ ...
  21  22  130  230  50  1  1.083  4  1  0;
 ];
Fault.con = [ ...
  22  115  230  50  1  1.083  0  0.001;
 ];
SW.con = [ ...
  29 100  13.8  1.2  0.8  9.9  -9.9 1.1 0.9  0.8 1 1 1;
  ];
PV.con = [ ...
  25 115  15    1.63  1.025  9.9  -9.9 1.1 0.9 1  1;
  26 61  13.8  1.54  1.026  9.9  -9.9 1.1 0.9 1  1;
  27 95  15    1.09  1.025  9.9  -9.9 1.1 0.9 1  1;
  28 150  13.8  1.01  1.025  9.9  -9.9 1.1 0.9 1  1;
  30 130  13.8  1.09  1.027  9.9  -9.9 1.1 0.9 1  1;
  ];
PQ.con = [ ...
   1 115 400 0.9 0.45 1.1 0.9 1  1;
   3 115 230 0.8 0.5 1.1 0.9 1  1;
   4 130 230 0.9 0.56 1.1 0.9 1  1;
   7 130 230 1.24 0.36 1.1 0.9 1  1;
   8 130 230 1.02 0.37 1.1 0.9 1  1;
   9 115 230 1.23 0.38 1.1 0.9 1  1;
  12 115 230 1.09 0.49 1.1 0.9 1  1;
  13 115 230 1.01 0.47 1.1 0.9 1  1;
  15 95 230 1.24 0.58 1.1 0.9 1  1;
  16 95 230 1.07 0.32 1.1 0.9 1  1;
  18 95 230 0.9  0.52 1.1 0.9 1  1;
  20 150 230 0.9  0.34 1.1 0.9 1  1;
```

```
  21 150 230 0.8  0.25 1.1 0.9 1  1;
  23 100 230 0.9  0.35 1.1 0.9 1  1;
  24 95 230 0.9  0.46 1.1 0.9 1  1;
  ];

Areas.con = [ ...
   1 0 1 0 0 0 0 0;
  ];

Bus.names = { ...
  'Bus 1'; 'Bus 2'; 'Bus 3'; 'Bus 4'; 'Bus 5';
  'Bus 6'; 'Bus 7'; 'Bus 8'; 'Bus 9'; 'Bus 10';
  'Bus 11'; 'Bus 12'; 'Bus 13'; 'Bus 14'; 'Bus 15';
  'Bus 16'; 'Bus 17'; 'Bus 18'; 'Bus 19'; 'Bus 20';
  'Bus 21'; 'Bus 22'; 'Bus 23'; 'Bus 24'; 'Bus 25';
  'Bus 26'; 'Bus 27'; 'Bus 28'; 'Bus 29'; 'Bus 30'};

Areas.names = { ...
  '30BUS'};
```

DECLARATION

I, the undersigned, declare that this thesis work is my original work, has not been presented for a degree in any other university and that all source of material used for the thesis have been fully acknowledged.

Mehari Mekuriaw Mengistie _____

Name Signature

Place: Addis Ababa Institute of Technology, Addis Ababa University, Addis Ababa

Date of Submission: July 5, 2015

This thesis has been submitted for examination with my approval as an advisor.

Dr. Solomon Kidane _____

Advisor‘s Name Signature